Improvement of direct electron transfer-type bioelectrocatalytic property of D-fructose dehydrogenase by protein engineering approach

Yuya Hibino

2019

Table of contents

General introduction

Bioelectrocatalysis is the conjugation of enzymatic redox reaction and electrode reaction [1-11]. It has been considerable interested in construction of biofuel cells and biosensors. Biofuel cells and biosensors are types of fuel cell or an electrochemical sensor that utilize enzymes or intact cells as the electrocatalysts. There are two types of bioelectrocatalysis: mediated electron transfer type and direct electron transfer- (DET-) type. The DET-type bioelectrocatalysis is expected to be utilized for construction of simple biofuel cells and biosensors [12, 13]. However, the DET-type bioelectrocatalysis has been reported in only limited numbers of enzymes.

In DET-type bioelectrocatalysis reactions, enzymes usually adsorb on an electrode surface and the active sites such as cofactors or prosthetic groups communicates electrochemically with an electrode. Generally, the active sites of redox enzymes are covered by insulating protein, and cannot communicate electrochemically with an electrode (Fig. 1 (A)) [14]. However, it is reported that in the limited numbers of redox enzymes, the redox active sites locate near the surface of enzymes, and communicate electrochemically with electrode. In this case, the tunnel (long-range) electron transfer occurs between the active sites and an electrode [2, 15, 16]. The interfacial electron transfer rate constant decreases exponentially with the distance between the electrode surface and the redox active site. If the distance extends 0.5 Å, the electron transfer rate constant becomes one-half [17]. In general, enzyme size is nano-meter order. Therefore, the adsorption orientation of enzymes is very important for DET-type bioelectocatalysis (Fig. 1 (B))[2, 15, 16].

In this study, the author focused on an enzyme D-fructose dehydrogenase (FDH) from *Gluconobacter japonicus* NBRC3260 [18, 19]. FDH was a membrane-bound enzyme that firstly discovered and purified by Ameyama in 1981 [20]. FDH catalyzes oxidation of D-fructose into 5-keto-D-fructose and show large anodic current in DET-type bioelectrocatalysis. Therefore, FDH is expected for construction D-fructose biofuel cells [21]. FDH is a heterotrimeric enzyme with a molecular mass of *ca*. 140 kDa, that consists of subunits I (67 kDa), II (50 kDa), and III (20 kDa) [22]. Subunit I has a flavin adenine dinucleotide (FAD) and subunit II has three heme *c* moieties as prosthetic groups. Subunit III plays a significant role in the expression of FDH. The crystal structure of FDH is undetermined (Fig. 2).

Investigation for DET-type bioelectrocatalysis of FDH gives rise to valuable information about discovery of new DET active enzyme, and realization of protein engineering method to enable DET-type bioelectrocatalysis. Past investigations have focused on the behaviors of FDH on an electrode and the electron transfer pathway in FDH. In order to research the behaviors of FDH, Sugimoto et al. characterized FDH adsorbed on self-assembled monolayer (SAM)-modified Au electrode. As a result, 2-mercaptoethanol that is added in enzyme solution for stabilization and
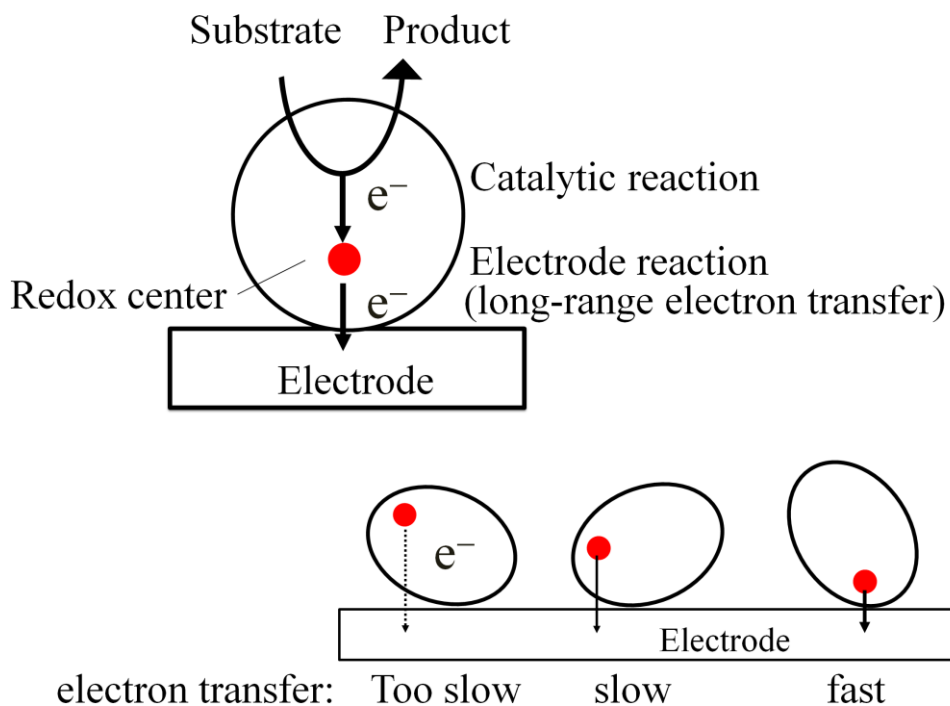
Figur 1. Schemes of (A) a model of the direct electron transfer pathway and (B) the effects of the adsorption orientation of enzymes on the distance between the electrode surface and the redox active site and the interfacial electron transfer rate constant.

solubilization of FDH respectively are adsorbed on Au electrode and plays a significant role in the stabilization of adsorbed FDH [23].

For research of the electron transfer pathway in FDH, Kawai et al. constructed and purified subunit I/III and subunit II. Subunit I/III exhibited FDH activity, and lost DET-type bioelectrocatalytic activity. However, a mixture of subunit I/III and subunit II exhibited FDH activity and DET-type bioelectrocatalytic activity. This results mean that D-fructose is oxidized at subunit I (FAD subunit) and the electron donating site is subunit II (heme c subunit). Additionally, Kawai et al. determined redox potentials of heme c moieties by spectroelectrochemical method. As a result, it is suggested that the one of three heme c moieties is not involved in the DET-type bioelectrocatalysis [24].
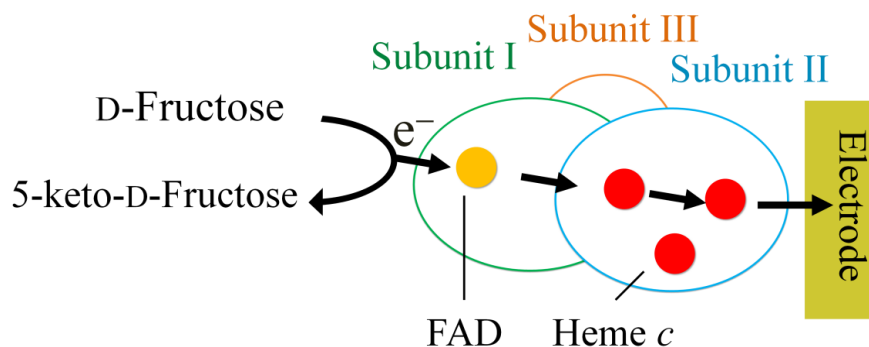
Figure 2 Scheme of FDH and model of electron transfer pathway in DET-type bioelectrocatalysis according to previous researches.

Subunit II of FDH has C-terminal hydrophobic region (CHR) expected by SOSUIsignal. This region is expected to play a role for anchoring to membranes. According to previous researches, FDH cannot catalyze direct electron transfer to electrode without subunit II. Therefore, it was expected that CHR may play some role in the DET-type biolectrocatalysis of FDH. However, the variant ΔchrFDH that lacks of CHR show clear DET-type activity. Therefore, CHR does not play a significant role in DET-type bioelectrocatalysis. Additionally, it is suggested that CHR is mainly involved in a binding process of subunit I/III and II [25].

FDH can be used for an anodic catalyst of a biofuel cell. A high power density (2.6 mW cm^{-2}) DET-type biofuel cell using FDH on the anode was reported [26]. However, if FDH catalyzes DET-type D-fructose oxidation in larger catalytic current density and more negative electrode potential, the power density increases remarkably.

FDH can be utilized for D-fructose biosensor. However, biosensors usually need to be operated at about 0 V (vs. Ag|AgCl|sat.KCl) in order to eliminate noise currents corresponding to directly redox reaction by an electrode such as reduction of oxygen or oxidation of ascorbic acid. In DET-type bioelectrocatalysis of FDH, the catalytic current at 0 V is very small; therefore FDH is not suitable for the measurement at 0 V.

In this study, in order to investigate the electron transfer pathway in FDH and improve DET-type bioelectrocatalysis of FDH, the author modified FDH by protein engineering method and characterized the variants.

In chapter1, the author constructed the variants (M301Q, M450Q, M578Q) in which the sixth axial ligand of the native heme c methionine (Met) ligand was replaced with glutamine (Gln). Since, Gln exhibits stronger electron-donating character than Met, the replacement may cause a shift in the formal potential ($E^{\circ\prime}$) of the heme c in the negative direction. As a result, M450Q catalyzes D-fructose oxidation in about 0.2 V low electrode potential. Additionally, it is suggested that the electrons accepted at the FAD in subunit I are transferred to electrodes via heme $3c$ and heme $2c$ in

subunit II without going through heme 1c (in this study, the heme c moieties are called heme 1c, 2c, 3c from N- to C-terminus).

In chapter2, the author constructed a variant that lacks 143 amino acid residues involving the heme 1c moiety on the N-terminus of subunit II (Δ1cFDH). Δ1cFDH exhibited clear DET-type catalytic activity, and the half wave potential was almost identical. Therefore, heme 1c does not play a role in DET-type bioelectrocatalytic reaction. Additionally, Δ1cFDH catalyzed D-fructose oxidation in larger DET-type catalytic currents than FDH. It is expected that the current increase is corresponding to an increase in the surface concentration of downsized enzymes.

In chapter3, the author constructed a variant (M450QΔ1cFDH) in which 143 amino acid residues involving heme 1c were removed and M450 as the sixth axial ligand of heme 2c was replaced with glutamine. M450QΔ1cFDH-adsorbed electrode exhibited a large limited current density and a negative direction shift in the half-wave potential ($E_{1/2}$) compared to that at the recombinant (native) FDH-adsorbed electrode. In addition, it is suggested that the M450QΔ1cFDH and M450Q is rather adsorbed in orientations suitable for DET-type bioelectrocatalysis.

In chapter4, the author successfully constructed the Δ1c2cFDH variant that lacks 199 amino acid residues including heme 1c and 2c. Δ1c2cFDH-adsorbed Au electrodes showed a clear DET-type catalytic current of D-fructose oxidation. In the DET reaction of Δ1c2cFDH, the electrons were transferred from the reduced FAD to the electrode via heme 3c. The interfacial electron transfer kinetics was improved probably by shortening the distance between heme c and the electrode. However, the limited current density decreased, which is opposite to what we expected from the downsizing mutation.

References

[1]   S.V. Hexter, T.F. Esterle, F.A. Armstrong, A unified model for surface electrocatalysis based on observations with enzymes, Phys. Chem. Chem. Phys. 16 (2014) 11822

[2]   C. Léger, P. Bertrand, Direct electrochemistry of redox enzymes as a tool for mechanistic studies, Chem. Rev. 108 (2008) 2379.

[3]   R.D. Milton, S.D. Minteer, Direct enzymatic bioelectrocatalysis: differentiating between myth and reality, J. R. Soc. Interface, 14 (2017) 0253.

[4]   N. Mano, A. de Poulpiqet, O2 reduction in enzymatic biofuel cells, Chem. Rev., 118 (2018) 2392.

[5]   D. Leech, P. Kavanagh, W. Schuhmann, Enzymatic fuel cells: recent progress, Electrochim. Acta. 84 (2012) 223.

[6]   S.C. Barton, J. Gallaway, P. Atanassov, Enzymatic biofuel cells for implantable and microscale devices, Chem. Rev. 104 (2004) 4867.

[7]   S. Shleev, J. Tkac, A. Christenson, T. Ruzgas, A.I. Yaropolov, J.W. Whittaker, L. Gorton, Cellobiose dehydrogenase modified electrodes: advances by materials science and biochemical engineering, Anal. Bioanal. Chem. 405 (2013) 3637.

[8]   N. Mano, L. Edembe, Bilirubin oxidases in bioelectrochemistry: Features and recent findings, Biosens. Bioelectron. 50 (2013) 478

[9]   M. Sensi, M. del Barrio, C. Baffert, V. Fourmond, C. Léger, New perspectives in hydrogenase direct electrochemistry, Curr. Opin. Electrochem. 5 (2017) 135.

[10]   I. Mazurenko, X. Wang, A. de Poulpiquet, E. Lojou, H2/O2 enzymatic fuel cells: from proof-of-concept to powerful devices, Sustainable Energy Fuels, 1 (2017) 1475.

[11]   K. Sakai, H. Xia, Y. Kitazumi, O. Shirai, K. Kano, Assembly of Direct-Electron-Transfer-Type Bioelectrodes with High Performance, Electrochim. Acta. 271 (2018) 271.

[12]   W. Zhang, G. Li, Third-generation biosensors based on the direct electron transfer of proteins, Anal. Aci. 20 (2004) 603.

[13]   T. Ikeda, Bioelectrochemical studies based on enzyme-electrocatalysis, Electrochim. Acta. 82 (2012) 158.

[14]   A.A. Karyakin, Principles of direct (mediator free) bioelectrocatalysis, Bioelectrochemistry 88 (2012) 70.

[15]   C. Léger, A.K. Jones, S.P.J. Albracht, F.A. Armstrong, Effect of a dispersion of interfacial electron transfer rates on steady state catalytic electron transport in [NiFe]-hydrogenase and other enzymes, J. Phys. Chem. B 106 (2002) 13058.

[16]   C. Léger, A.K. Jones, W. Roseboom, S.P.J. Albracht, F.A. Armstrong, Enzyme electrokinetics: hydrogen evolution and oxidation by *allochromatium vinosum* [NiFe]-hydrogenase, Biochemistry 41 (2002) 15736.

[17]   C.C. Moser, J.M. Keske, K. Warncke, R.S. Farid, P.L. Dutton, Nature of biological electron transfer, Nature of biological electron transfer, Nature 355 (1992) 796–802.

[18]   T. Ikeda, F. Matsushita, M. Senda, Amperometroc fructose sensor based on direct bioelectrocatalysis, Biosens. Bioelectron. 6 (1991) 299.

[19]   Y. Kamitaka, S. Tsujimura, N. Setoyama, T. Kajino, K. Kano, Fructose/dioxygen biofuel cell based on direct electron transfer-type bioelectrocatalysis, Phys. Chem. Chem. Phys. 9 (2007) 1793.

[20]   M. Ameyama, E. Shinagawa, K. Matsushita, O. Adachi, D-Fructose dehydrogenase of *gluconobacter industrius*: purification, characterization, and application to enzymatic microdetermination of D-fructose, J. Bacteriol. 145 (1981) 814.

[21]   Y. Kamitaka, S. Tsujimura, K. Kano, High current density bioelectrolysis of D-fructose at fructose dehydrogenase-adsorbed and ketjen black-modified electrodes without a mediator,

Chem. Lett. 36 (2007) 218.

[22]   S. Kawai, M. Tsutsumi, T. Yakushi, K. Kano, K. Matsushita, Heterologous overexpression and characterization of a flavoprotein-cytochrome *c* complex fructose dehydrogenase of *gluconobacter iapinicus* NBRC3260, Appl. Environ. Microbiol. 79 (2013) 1654.

[23]   Y. Sugimoto, Y. Kitazumi, O. Shirai, K. Kano, Role of 2-mercaptoethanol in direct electron transfer-type bioelectrocatalysis of fructose dehydrogenase at Au electrodes, Electrochim. Acta 170 (2015) 242.

[24]   S. Kawai, T. Yakushi, K. Matsushita, Y. Kitazumi, O. Shirai, K. Kano, The electron transfer pathway in direct electrochemical communication of fructose dehydrogenase with electrodes, Electrochem. Commun, 38 (2014) 28.

[25]   Y. Sugimoto, S. Kawai, Y. Kitazumi, O. Shirai, K. Kano, Function of C-terminal hydrophobic region in fructose dehydrogenase, Electrochim. Acta 176 (2015) 976.

[26]   K. So, S. Kawai, Y. Hamano, Y. Kitazumi, O. Shirai, M. Hibi, J. Ogawa, K. Kano, Improvement of a direct electron transfer-type fructose/dioxygen biofuel cell with a substrate-modified miocathode, Phys. Chem. Chem. Phys., 16 (2014) 4823.

Chapter1

Mutation of Heme *c* Axial Ligands in D-Fructose Dehydrogenase for Investigation of Electron Transfer Pathways and Reduction of Overpotential in Direct Electron Transfer-Type Bioelectrocatalysis

D-Fructose dehydrogenase (FDH), a flavoprotein-cytochrome *c* complex, exhibits high activity in direct electron transfer (DET)-type bioelectrocatalysis. One of the three heme *c* moieties in FDH is the electron-donating site to the electrodes, and another heme *c* is presumed to not be involved in the catalytic cycle. In order to confirm the electron transfer pathway, the author constructed three mutants in which the sixth axial methionine ligand (M301, M450, or M578) of one of the heme *c* moieties was replaced with glutamine, which was selected with the expectation that it would shift the formal potential of the heme *c* moieties in the negative direction. An M450Q mutant successfully reduced the overpotential by approximately 0.2 V, giving a limiting current close to that of the native FDH. In contrast, an M301Q mutant remained almost unchanged and an M578Q mutant drastically decreased DET-type catalytic activity. The results indicate that the electron transfer in the native FDH occurs in sequence from the flavin, through the heme *c* with M578, to the heme *c* with M450 (as the electron-donating site to the electrodes), without going through the heme *c* with M301. The M450Q mutant will be useful for biofuel cells because of the decreased overpotential.

Introduction

Bioelectrocatalysis is an electrode reaction coupled with a redox enzymatic reaction, which is useful for the construction of bioelectrochemical devices such as biofuel cells and biosensors, and for fundamental research into the electron transfer reactions of enzymes. The electrode reactions are classified into two types: direct electron transfer (DET)-type bioelectrocatalysis and mediated electron transfer (MET)-type bioelectrocatalysis [1-7]. In particular, DET-type bioelectrocatalysis is valuable for use in constructing simple bioelectrochemical devices and in minimizing thermodynamic energy losses in bioelectrocatalysis [1,2].

D-Fructose dehydrogenase (FDH) from *Gluconobacter japonicus* NBRC 3260 is a membrane-bound heterotrimeric enzyme comprising subunits I (67 kDa), II (50 kDa), and III (20 kDa) [8]. Subunit I has a flavin adenine dinucleotide (FAD) while subunit II has three heme *c* moieties as prosthetic groups [9]. FDH exhibits high activity in DET-type bioelectrocatalytic oxidation of D-fructose, and is useful for the construction of DET-type biosensors and biofuel cells [10,11]. In previous research, it was pointed out that the FAD oxidizes D-fructose into 5-keto-D-fructose, one of the three heme *c* moieties is the electron-donating site to the electrode, and

another heme c is not involved in the DET-type catalytic cycle [12].

Determination of the electron transfer pathway of DET-type bioelectrocatalysis of FDH gives rise to valuable information about improving the redox properties of FDH. Although the crystal structure of FDH remains unknown, the author attempted to identify the heme c acting as the electron-donating site as well as the non-catalytic heme c by utilizing a protein engineering technique. Glutamine (Gln) exhibits stronger electron-donating character than methionine (Met) as the axial ligand of the native heme c. Therefore, the replacement of the natural axial Met ligand with Gln can be expected to cause a shift in the formal potential ($E^{\circ\prime}$) of the corresponding heme c in the negative direction [13], as demonstrated in the mutation of the axial ligand of type I copper in a multicopper oxidase, bilirubin oxidase [14]. The author's hypothesis in this work is that a Gln mutation of the axial Met ligand of the electron-donating heme c site will cause a negative shift in the half-wave potential ($E_{1/2}$) of the DET-type sigmoidal catalytic wave; however, practically no change is expected for a Gln mutation of the axial Met ligand of the non-catalytic heme c. A negative shift in $E_{1/2}$ of the DET-type catalytic wave indicates a decrease in the overpotential of FDH-catalyzed fructose oxidation, which could be used to improve the performance of fructose/O_2 biofuel cells. Additionally, if the DET-type activity around 0 V (vs. Ag|AgCl|sat.KCl), D-fructose biosensor can eliminate noise currents corresponding to directly redox reaction by an electrode such as reduction of oxygen or oxidation of ascorbic acid.

In this work, the author constructed three mutants in which the sixth axial Met ligand (M301, M450, or M578) of one of the three types of heme c was replaced with Gln (Fig. 1). The effects of the mutation on the catalytic waves were examined with cyclic voltammetry. The three heme c moieties coordinated by M301, M450, and M578 as the axial ligands are called heme $1c$, heme $2c$, and heme $3c$, respectively. The three mutants exhibited significant differences in voltammograms. In particular, an M450Q mutation on heme $2c$ significantly reduced the overpotential of the DET-type bioelectrocatalytic wave by approximately 0.2 V. On the basis of the changes in the catalytic waves caused by the mutations, the author proposes the most likely electron transfer pathway in the native FDH.
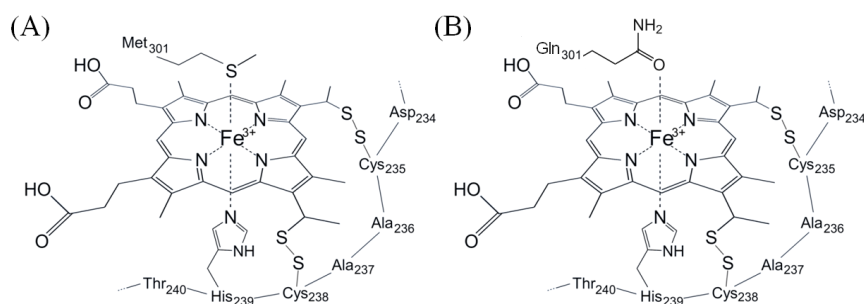

Fig. 1. Schematic drawings of (A) heme $1c$ and (B) heme $1c$ in which Met301 is replaced with Gln

Chapter 1

Experimental

Materials

Potassium ferricyanide was purchased from Nakalai Tesque (Japan). Other chemicals were acquired from Wako Pure Chemical Industries (Japan).

Preparation of the mutants and FDH

The author performed site-directed mutagenesis by inverse polymerase chain reactions to prepare M301Q, M450Q, and M578Q mutants. The plasmid pSHO13 [9] harboring the complete FDH$_{ATG}$ gene was used for expressing the mutants.

To prepare the M301QFDH, M450QFDH, and M578QFDH variants, the author performed site-directed mutagenesis with pSHO13 that was used for expressing the recombinant (native) FDH [9]. pSHO13 is a broad-host-range vector pBBR1-MCS4 [20] inserted with a fragment of a putative promoter region of the *adhAB* gene of *G. oxydans* 621H and a fragment of the complete *fdh*$_{ATG}$ gene. The site-directed mutation was introduced to the plasmid by replacing one of the ATG codons corresponding to Met301, Met450, or Met578 by the CAG codon (corresponding to Gln). The site-directed mutation M301Q, M450Q and M578Q were introduced to the *fdh* gene by inverse polymerase chain reaction (PCR) using primers fdhC_heme1*c*Gln(+) (5′-CCAGCCTTATGACGCTT ACAATC-3′) and fdhC_heme1*c*(−) (5′-AGGATTTCGTGGTTATCCGTTGTGC-3′), fdhC_heme2*c*Gln(+) (5′-ACAGGCAGAAGCAATCGAGCATAGCC-3′) and fdhC_heme2*c*(−) (5′-GGTCCTGCTGCACGAGCATGTG-3′), fdhC_heme3*c*Gln(+) (5′-GCAGCCGGCTTTTGGTCC AGACTCTCTCG-3′) and fdhC_heme3*c*(−) (5′-AGGATTTCGTGGTTATCCGTTGTGC-3′) respectively. In order to avoid some risks of wrong copies at the vector in inverse PCR, pSHO13 was treated with HindIII and BamHI, and almost all *fdh*$_{ATG}$ gene was inserted into pT7Blue, which was treated with HindIII and BamHI, and then the inverse PCR was performed. All nucleotide sequences of the mutated *fdh*$_{ATG}$ gene of PCR products were confirmed by Fasmac sequencing service (Japan). The fragment of mutated *fdh*$_{ATG}$ gene was treated with HindIII and BamHI, and inserted into pSHO13 that was treated with HindIII and BamHI to yield pYUF9, pYUF17 and pYUF25. pYUF9, pYUF17 and pYUF25 were used for expression of FDH variants. *G. oxydans* NBRC 12528 Δ*adhA*::Km^r was transformed with pYUF9, pYUF17 and pYUF25, as described in a previous paper[35].

The concentration of recombinant (native) FDH and the mutants were spectrophotometically determined using an adsorption coefficient of heme *c* at 550 nm ($\varepsilon_{550} = 23{,}000$ M^{-1}cm^{-1}; M = mol dm^{-3} [15]).

strain	Description	Source or reference
Escherichia coli		
DH5α	F⁻*endA1hsdR17(r$_k$⁻m$_k$⁺) supE44thi-1λ⁻recAlgyrA96relA1 deoRΔ(lacZYA-argF)*U169Φ80d*lacZ*ΔM15	[16]
HB101	F⁻*thi-1 hsdS20*(r$_B$m$_B$)*supE44recA13ara14leuB6proA2 lacY1galK2rpsL20*(Str^r*xyl-5 mtl-1λ*⁻)	[17]
Gruconobacter oxydans		
NBRC12528 ΔadhA mutant	NBRC12528 Δ*adh*A::Km^r	[18]

Plasmid	Description	Source or reference
pKR2013	Plasmid mediates plasmid transfer; Km^r	[19]
pT7Blue	General purpose cloning vector	Novagen
pBBR1MCS-4	Broad-host-range plasmid; *mob* Ap^r	[20]
pSHO13	pBBR1MCS-4,a 3.7-kb fragment of the *fdh$_{ATG}$* genes, a 0.7-kb fragment a putative promoter region of the *adhAB* gene of *G*.oxydans621H	[9]
pYUF9	pBBR1MCS-4,a 3.7-kb fragment of the *fdh$_{ATG}$* genes carrying M301Q mutation, a 0.7-kb fragment a putative promoter region of the *adhAB* gene of *G*.oxydans621H	This study
pYUF17	pBBR1MCS-4,a 3.7-kb fragment of the *fdh$_{ATG}$* genes carryingM450Q mutation, a 0.7-kb fragment a putative promoter region of the *adhAB* gene of *G*.oxydans621H	This study
pYUF25	pBBR1MCS-4,a 3.7-kb fragment of the *fdh$_{ATG}$* genes carrying M578Q mutation, a 0.7-kb fragment a putative promoter region of the *adhAB* gene of *G*.oxydans621H	This study

Table 1. Bacterial strains and plasmids used in this study

Electrochemical measurements

Cyclic voltammetry was performed in a McIlvain buffer (pH 4.5) at 25 °C on an ALS 611s voltammetric analyzer under anaerobic conditions. The working electrode was an Au electrode. The Au electrode was polished to a mirror-like finish with Al_2O_3 powder (0.05-μm particle size), rinsed with distilled water, and sonicated in distilled water. The reference and counter electrodes were a handmade Ag|AgCl|sat.KCl electrode and a Pt wire, respectively. Here, all potentials are referred to the reference electrode. All electrochemical measurements were performed in 1.0 mL of McIlvain

buffer (pH 4.5) containing 0.1 M D-fructose under anaerobic conditions at a scan rate of 10 mV s^{-1}. In measurements of bioelectrocatalytic currents, 3 µL each of the enzyme stock solutions (recombinant (native) FDH: 28 µM, M301Q: 17 µM, M450Q: 15 µM, M578Q: 16 µM) was added to the buffer solution.

Other analytical methods

FDH activity was measured photometrically with potassium ferricyanide (as an electron acceptor) and the ferric dupanol reagent, as described in ref. [8]. One FDH unit was defined as the amount of enzyme oxidizing 1 µmol of D-fructose per min at pH 4.5. The protein concentration was determined with a DC protein assay kit (Bio-Rad, CA) using bovine serum albumin as a standard.

Result and discussion

Fig. 2 (A) shows cyclic voltammograms of recombinant (native) FDH- and M450Q mutant-adsorbed Au electrodes in the presence of D-fructose. Each of the enzyme was physically adsorbed on a bare Au electrode from an electrolysis solution containing the corresponding enzyme. Clear DET-type catalytic waves corresponding to fructose oxidation were observed at both of the enzyme-adsorbed electrodes. The current-potential curves were not affected by stirring. Therefore, the catalytic current is controlled by the enzyme kinetics and the interfacial electron transfer kinetics alone [15,21-23]. The current approached a limiting value at 0.5 V at the M450Q mutant-adsorbed electrode. The limiting catalytic current (I_{lim}; to be observed at more positive potentials) is completely controlled by the enzyme kinetics [15, 21-23]:

$$I_{\text{lim}} = n_{\text{s}}FAk_{\text{cat}}\Gamma_{\text{eff}} \qquad\qquad (1)$$

where n_{E} is the number of electrons in one catalytic turnover of enzyme, F is the Faraday constant, A is the electrode surface area, k_{cat} is the catalytic constant, and Γ_{eff} is the surface concentration of enzyme. It can be assumed that the surface concentrations of the enzymes are almost identical with each other under these experimental conditions, as evidenced by quartz crystal microbalance measurements for other FDH mutants [21]. In order to discuss k_{cat} in Eq. (1), it is important to record I_{lim} at sufficiently positive potentials. However, measurements at potentials more positive than 0.5 V cause a decrease in the catalytic current because of the formation of an Au oxide layer [21]. In reality, when the potential was scanned up to 0.7 V, the current decreased gradually during the multiple scans, as shown in Fig. 3. Such a decrease in the current was not observed in multi-scan voltammograms up to 0.5 V. Therefore, the author tentatively uses the catalytic current at 0.5 V ($I_{0.5\text{ V}}$) as a surrogate for I_{lim}. $I_{0.5\text{ V}}$ of the M450Q mutant-adsorbed electrode was close to that of the recombinant (native) FDH-adsorbed electrode; however, it is not ruled out that the M450Q mutant-adsorbed electrode exhibits a somewhat smaller I_{lim} compared with the recombinant (native) FDH-adsorbed electrode at sufficiently positive potentials. This means that the M450Q mutation
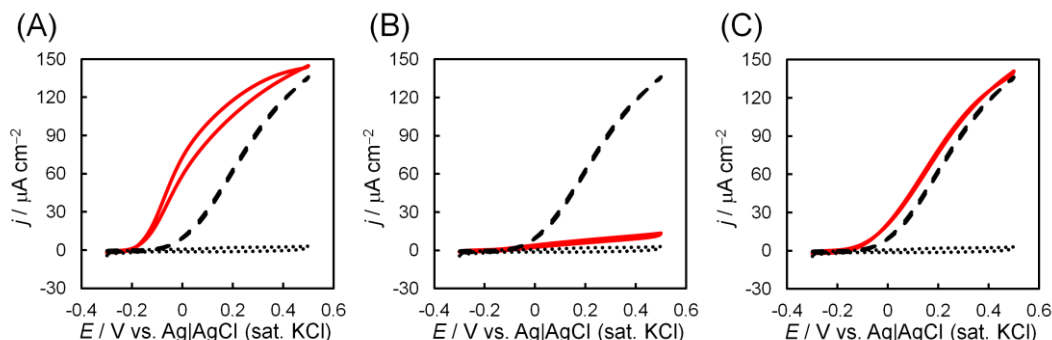
Figure 2. Cyclic voltammograms of D-fructose oxidation at (A-C: broken line) a recombinant (native) FDH-adsorbed Au electrode and (solid lines) (A) M450Q, (B) M578Q, and (C) M301Q mutant adsorbed Au electrodes in a McIlvain buffer (pH 4.5) containing 0.1 M D-fructose under anaerobic conditions at a scan rate of 10 mV s^{-1}. The dotted lines indicate a background voltammogram at a bare Au electrode.
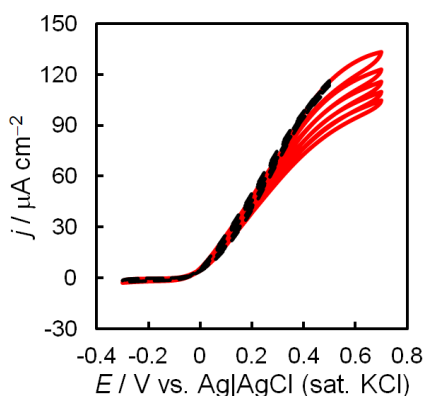

Figure 3. Multi-scan cyclic voltammograms of D-fructose (0.1 M) at an recombinant (native) FDH-adsorbed Au electrode in a McIlvain buffer (pH 4.5) containing 0.1 M D-fructose under anaerobic conditions at a scan rate of 10 mV s^{-1}.   The broken line indicates a multi-can cyclic voltammogram in the potential range from –0.3 V to 0.5 V.

does not significantly affect k_{cat} or causes only a small decrease in k_{cat}, if any.

In contrast, the onset potential at which an anodic wave starts to appear shifted negatively at the M450Q mutant-adsorbed electrode. Here the author will tentatively define the apparent half-wave potential ($E_{1/2,app}$) as the potential at which $I = I_{0.5\,V}/2$. $E_{1/2,app}$ was shifted by approximately 0.2 V in the negative direction by the M450Q mutation. In the case of type I copper in bilirubin oxidase also, the replacement of the axial Met ligand with Gln caused a potential shift in $E^{\circ\prime}$ by 0.23 V in the negative direction [14]. All these results strongly suggest that heme 2c is the

electron-donating site, and that the M450Q mutation causes a negative shift in $E^{\circ\prime}$ of heme $2c$, as illustrated in Fig. 4. This negative shift has the big advantage of decreasing the overpotential of the DET-type bioelectrocatalytic oxidation of D-fructose, which will be important to improve the performance of FDH-based biofuel cells. The small decrease in k_{cat} by the mutation (if any) may be ascribed to the negative shift in $E^{\circ\prime}$ of heme $2c$, because the shift may result in a decrease in the electron transfer rate constant due to a decreased driving force.

The M450Q mutant exhibited a low activity for D-fructose oxidation in solution (150 ± 30 U mg^{-1}) compared with recombinant (native) FDH (300 ± 50 U mg^{-1}) when measured with $K_3[Fe(CN)_6]$ as an electron acceptor. Heme $2c$ is likely the electron-donating site for transfer to a soluble electron acceptor in solution as well as to the electrode. Therefore, the decrease in the solution activity seems to be ascribed in part to the negative shift in $E^{\circ\prime}$ of heme $2c$.However, the decrease in the solution activity is large in extent compared with the decrease in the DET-type bioelectrocatalytic activity. It should be noted here that the catalytic constant as a solution activity has a definition different from that of k_{cat} in Eq. (1) and reflects the interaction between the enzyme and an electron acceptor. Therefore, the catalytic constant in solution is not necessarily correlated with k_{cat}. The M450Q mutation seems to partly disturb electron transfer to $[Fe(CN)_6]^{3-}$ (e.g., because of possible mutation-induced electrostatic repulsion or steric hindrance). In contrast, long-range electron transfer kinetics in DET-type bioelectrocatalysis does not seem to be sensitive to the M450Q mutation.

As shown in Fig. 2 (B), an M578Q mutant-adsorbed electrode also exhibited a DET-type catalytic anodic wave in the presence of fructose. However, the catalytic current density was extremely low compared with that at the recombinant (native) FDH-adsorbed electrode. The D-fructose oxidation activity of the M578Q mutant was also very low (10 ± 4 U mg^{-1}) in solution. The M578Q mutation likely causes a negative shift in the $E^{\circ\prime}$ of heme $3c$, as illustrated in Fig. 4, and the potential shift seems to interfere with intermolecular electron transfer from the reduced FAD to heme $3c$ because of a decreased driving force.

As shown in Fig. 2 (C), an M301Q mutant-adsorbed electrode exhibited a clear DET-type catalytic anodic wave. The shape and the intensity were very close to those of the recombinant (native) FDH-adsorbed electrode. The M301Q mutation caused a negative shift in $E_{1/2,app}$ by only 0.05 V. In addition, D-fructose oxidation activity in solution remained almost unchanged by the mutation (220 ± 10 U mg^{-1}). Therefore, the author can safely conclude that heme $1c$ is not involved in the catalytic reaction, as illustrated in Fig. 4. Because the three heme c moieties are located closely in subunit II of FDH, it is likely that the M301Q mutation slightly affects the situation of heme 2c, which results in a small negative shift in $E^{\circ\prime}$ of heme 2c. This seems to be responsible for the small negative shift in $E_{1/2,app}$ by the M301Q mutation.
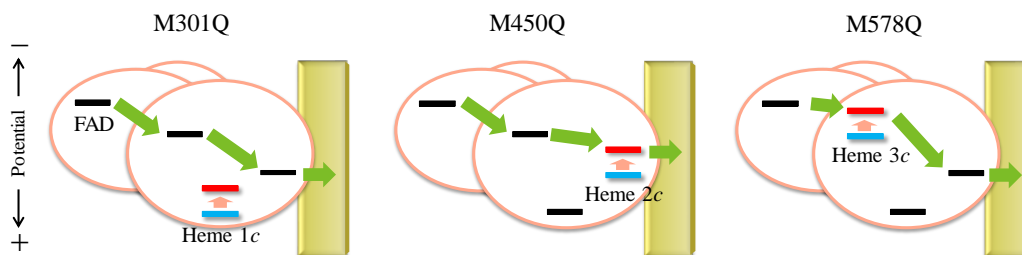
Figure 4. Cartoons of electron transfer in the three mutants

Conclusion

In this work, the author successfully constructed the three mutants M301Q, M450Q, and M578Q. The M450Q mutant can reduce the overpotential of catalytic D-fructose oxidation. The mutant will be useful for FDH-based DET-type biofuel cells to increase the operation voltage. Additionally, this variant is useful for construction noiseless biosensor. Another very important conclusion is that the electron transfer in the recombinant (native) FDH occurs from the FAD to heme 2c with M450 as the sixth axial ligand, via heme 3c with M578, without going through heme 1c with M301. Heme 2c with M450 is considered to be the electron-donating site to the electrode. This conclusion is in agreement with that reported in previous paper [12].

References

[1]   J.A. Cracknell, K.A. Vincent, F.A. Armstrong, Enzymes as working or inspirational electrocatalysts for fuel cells and electrolysis, Chem. Rev. 108 (2008) 2439.

[2]   C. Léger, P. Bertrand, Direct electrochemistry of redox enzymes as a tool for mechanistic studies, Chem. Rev. 108 (2008) 2379.

[3]   M.J. Moehlenbrock, S.D. Minteer, Extended life time biofuel cells, Chem. Soc. Rev. 37 (2008) 1188.

[4]   N. Mano, F. Mao, A. Heller, A miniature membrane-less biofuel cell operating at +0.60 V under physiological conditions, ChemBioChem 5 (2004) 1703.

[5]   D. Leech, P. Kavanagh, W. Schuhmann, Enzymatic fuel cells: recent progress, Electrochim. Acta 84 (2012) 223.

[6]   S.C. Barton, J. Gallaway, P. Atanassov, Enzymatic biofuel cells for implantable and microscale devices, Chem. Rev. 104 (2004) 4867.

[7]   R. Ludwig, W. Harreither, F. Tasca. L. Gorton, Cellobiose dehydrogenase: a versatile catalyst

for electrochemical applications, ChemPhysChem 11 (2010) 2674.

[8]   M. Ameyama, E. Shinagawa, K. Matsushita, O. Adachi, D-Fructose dehydrogenase of *gluconobacter industrius*: purification, characterization, and application to enzymatic microdetermination of D-fructose, J. Bacteriol. 145 (1981) 814.

[9]   S. Kawai, M. Tsutsumi, T. Yakushi, K. Kano, K. Matsushita, Heterologous overexpression and characterization of a flavoprotein-cytochrome *c* complex fructose dehydrogenase of *gluconobacter iapinicus* NBRC3260, Appl. Environ. Microbiol. 79 (2013) 1654.

[10]   T. Ikeda, F. Matsushita, M. Senda, Amperometroc fructose sensor based on direct bioelectrocatalysis, Biosens. Bioelectron. 6 (1991) 299.

[11]   Y. Kamitaka, S. Tsujimura, K. Kano, High current density bioelectrolysis of D-fructose at fructose dehydrogenase-adsorbed and ketjen black-modified electrodes without a mediator, Chem. Lett. 36 (2007) 218.

[12]   S. Kawai, T. Yakushi, K. Matsushita, Y. Kitazumi, O. Shirai, K. Kano, The electron transfer pathway in direct electrochemical communication of fructose dehydrogenase with electrodes, Electrochem. Commun, 38 (2014) 28.

[13]   G. Battistuzzi, M. Borsari, J.A. Cowan, A. Ranieri, M. Sola, Control of cytochrome *c* redox potential: axial ligation and protein environment effects, J. Am. Chem. Soc. 124 (2002) 5315.

[14]   Y. Kamitaka, S. Tsujimura, K. Kataoka, T. Sakurai, T. Ikeda, K. Kano, Effects of axial ligand mutation of the type I copper site in bilirubin oxidase on direct electron transfer-type bioelectrocatalytic reduction of dioxigen, J. Electroanal. Chem. 601 (2007) 119.

[15]   J. Marcinkeviciene, G. Johansson, Kinetic studies of the active sites functioning in the quinohemoprotein fructose dehydrogenase, FEBS Lett. 318 (1993)23-26.

[16]   S.G. Grant, J. Jessee, F.R. Bloom, D. Hanahan, Differential plasmid rescue from transgenic mouse DNAs into *Escherichia coli* methylationrestriction-mutants, *Proc. Natl. Acad. Sci. U. S. A.,* 87 (1990) 4645

[17]   H.W. Boyer, D. Roulland-Dussoix, A complementation analysis of the restriction and modification of DNA in *Escherichia coli,. J. Mol. Biol.,* 41 (1969) 459

[18]   H. Habe, Y. Shimada, T. Yakushi, H. Hattori, Y. Ano, T. Fukuoka, D. Kitamoto, M. Itagaki, K. Watanabe, H. Yanagishita, K. Matsushita, K. Sakaki, Microbial production of glyceric acid, an organic acid that can be mass produced from glycerol, *Appl. Environ. Microbiol.,* 75 (2009) 7760

[19]   D.H. Figurski, D.R. Helinski, Replication of an origin-containing derivative of plasmid RK2 dependent on a plasmid function provided in trans., *Proc. Natl. Acad. Sci. U. S. A.,* 76 (1979) 1648

[20]   M.E. Kovach, P.H. Elzer, D.S. Hill, G.T. Robertson, M.A. Farris, R.M. Roop, II, K.M. Petrson, Four new derivatives of the broad-host-range cloning vector pBBR1MCS carrying

different antibiotic-resistance cassettes, *Gene*, 166 (1995) 175

[21]   Y. Sugimoto, Y. Kitazumi, O. Shirai, K. Kano, Role of 2-mercaptoethanol in direct electron transfer-type bioelectrocatalysis of fructose dehydrogenase at Au electrodes, Electrochim. Acta 170 (2015) 242.

[22]   C. Léger, A.K. Jones, S.P.J. Albracht, F.A. Armstrong, Effect of a dispersion of interfacial electron transfer rates on steady state catalytic electron transport in [NiFe]-hydrogenase and other enzymes, J. Phys. Chem. B 106 (2002) 13058.

[23]   C. Léger, A.K. Jones, W. Roseboom, S.P.J. Albracht, F.A. Armstrong, Enzyme electrokinetics: hydrogen evolution and oxidation by *allochromatium vinosum* [NiFe]-hydrogenase, Biochemistry 41 (2002) 15736.

[24]   K. So, R. Hamamoto, R. Takeuchi, Y. Kitazumi, O. Shirai, R. Endo, H. Nishihara, Y. Higuchi, K. Kano, Bioelectrochemical analysis of thermodynamics of the catalytic cycle and kinetics of the oxidative inactivation of oxygen-tolerant [NiFe]-hydrogenase, J. Electroanal. Chem. 766 (2016) 152.

[25]   H. Xia, Y. Kitazumi, O. Shirai, K. Kano, Enhanced direct electron transfer-type bioelectrocatalysis of bilirubin oxidase on negatively charged aromatic compound-modified carbon electrode, J. Electroanal. Chem. 763 (2016) 104.

Chapter2

Construction of a Protein-Engineered Variant of D-Fructose Dehydrogenase for Direct Electron Transfer-Type Bioelectrocatalysis

D-Fructose dehydrogenase (FDH), a heterotrimeric membrane-bound enzyme, exhibits strong activity in direct electron transfer- (DET-) type bioelectrocatalysis. believes that the electrons that are accepted at the flavin adenine dinucleotide (FAD) catalytic center in subunit I are transferred to electrodes via two of the three heme c moieties in subunit II without going through the other heme c moiety (called heme $1c$). In this study, the author constructed a variant that lacks 143 amino acid residues involving the heme $1c$ moiety on the N-terminus of subunit II ($\Delta 1c$FDH), and the author characterized the bioelectrocatalytic properties of $\Delta 1c$FDH using cyclic voltammetry. A clear DET-type catalytic oxidation wave of D-fructose was observed at the $\Delta 1c$FDH-adsorbed Au electrodes. The result clearly verifies our assumption. In addition, the limiting current density of $\Delta 1c$FDH was one and a half times larger than that of the recombinant (native) FDH in DET-type bioelectrocatalysis. The downsizing protein engineering causes an increase in the surface concentration of the electrochemically effective enzymes and an improvement in the heterogeneous electron transfer kinetics.

Introduction

Direct electron transfer- (DET-) type bioelectrocatalysis involves coupling of redox enzymatic reactions and electrode reactions without mediators [1–9]. DET-type bioelectrocatalysis is attracting significant attention for the construction of mediator-free biosensors and biofuel cells and for the fundamental analysis of redox properties of enzymes [1, 2, 10, 11]. In DET-type bioelectrocatalysis, it is important that the redox active site of an enzyme is located near the surface of the enzyme and that the enzyme is adsorbed in a proper orientation that is suitable for direct electrochemical communication. However, in most redox enzymes, the redox active site is embedded in insulating peptides. Therefore, only a limited number of redox enzymes exhibit clear DET-type bioelectrocatalytic activity [7, 8, 12-14].

The author has focused on D-fructose dehydrogenase (FDH) from *Gluconobacter japonicus* NCBR 3260 as a model enzyme with DET-type bioelectrocatalytic activity [15, 16]. FDH that is adsorbed on electrodes produces a catalytic wave of D-fructose oxidation at large current densities [17, 18]. FDH shows strict substrate specificity to D-fructose and is used in diagnosis and food analysis [19, 20]. A biofuel cell with the DET-type bioelectrocatalysis of FDH on the anode exhibited a high power density (2.6 mW cm^{-2}) [21]. FDH is a membrane-bound enzyme with a molecular mass of ca. 140 kDa. It is a heterotrimeric enzyme complex that consists of subunits I (67

17

kDa), II (51 kDa), and III (20 kDa) [22]. Subunit I has one flavin adenine dinucleotide (FAD), and subunit II has three heme c moieties [23]. In this work, the three heme c moieties are called heme $1c$, $2c$, and $3c$ from the N- to the C-terminus. FAD in FDH oxidizes D-fructose to 5-keto-D-fructose. It is presumed that the electron is transferred from the reduced FAD to heme $3c$, heme $2c$, and an electrode and that heme $1c$ is not involved in the DET-type catalytic cycle [24,25]. Therefore, it is important to construct a variant that lacks heme $1c$ to verify the author's assumption and to demonstrate a strategy of protein engineering to improve the DET-type bioelectrocatalytic activity.

In this study, the author constructed two variants ($\Delta 1c$-siteFDH and $\Delta 1c$FDH). In $\Delta 1c$-siteFDH, the sequences of heme $1c$ binding site "CAACH",in which two cysteines (Cys 235 and Cys238) and a heme c were covalently linked, was replaced with "AAAAH". $\Delta 1c$FDH lacks 143 amino acid residues and heme $1c$ on the N-terminus of subunit II (Fig. 1). The author's hypothesis is as follows. The FDH variants that lack heme $1c$ moietiy can catalyze DET-type bioelectorocatalysis reaction, because heme $1c$ is not involved in the DET-type reaction. Additionally, because the rate constant of the heterogeneous electron transfer ($k°$) increases exponentially with a decrease in the distance between the active sites of the enzyme and the electrode surface [26], heme $2c$ in FDH (as an electron-donating site to an electrode) may come close to the electrode surface via the proposed protein engineering, resulting in an increase in $k°$. Moreover, the protein engineering makes FDH compact and leads to an increase in the surface density of the enzyme monolayer on the electrode.

In cyclic voltammetry, the $\Delta 1c$FDH-adsorbed electrodes exhibited a large steady-state catalytic wave of D-fructose oxidation compared with recombinant (native) FDH-adsorbed electrodes. To date, several downsizing protein engineering approaches have been attempted, for example, for Cu efflux oxidase to delete a helical region [27] and for horseradish peroxydase [28], glucose oxidase [29] and cellobiose dehydrogenase   [30] for deglycosylation. However, this study is the first trial of the deletion of such a long region that includes one of the prosthetic groups to enhance the DET-type bioelectrocatalytic activity.

Experimental

Materials

Herculase II fusion DNA polymerase and restriction endonucleases were purchased from Agilent Technologies (Santa Clara, CA) and Takara Shuzo (Japan), respectively. DNA ligase was obtained from Toyobo (Japan). Potassium ferricyanide was obtained from Nacalai Tesque (Japan). Other chemicals were obtained from Wako Pure Chemical Industries (Japan).

Preparation of the Mutants and FDH

To prepare the $\Delta 1c$-siteFDH variants, the author performed site-directed mutagenesis with

pSHO13 that was used for expressing the recombinant (native) FDH [23]. pSHO13 is a

N−Terminal

MRYFRPLSATAMTTVLLLAGTNVRAQ<u>PTEPTPASAHRPSISRGHYLAIAAD</u>CAACHT
<u>NGRDGQFLAGGYAISSPMGNIYSTNITPSKTHGIGNYTLEQFSKALRHGIRADGAQL
YPAMPYDAYNRLTDEDVKSLYAYIMTEVKPVDAPSPKTQLPFPFSIRASLGIWKI</u>AAR
IEGKPYVFDHTHNDDWNRGRYLVDELAHCGECHTPRNFLLAPNQSAYLAGADIGS
WRAPNITNAPQSGIGSWSDQDLFQYLKTGKTAHARAAGPMAEAIEHSLQYLPDADI
SAIVTYLRSVPAKAESGQTVANFEHAGRPSSYSVANANSRRSNSTLTKTTDGAALYEA
VCASCHQSDGKGSKDGYYPSLVGNTTTGQLNPNDLIASILYGVDRTTDNHEILMPAF
GPDSLVQPLTDEQIATIADYVLSHFGNAQATVSADAVKQVRAGGKQVPLAKLASPGV
MLLLGTGGILGAILVVAGLWWLISRRKKRSA

C−Terminal

Figure 1. The amino acid sequences of subunit II. The underlined amino acid sequences were deleted. Three hatched amino acid sequences (CXXCH) are motifs for the heme *c* covalently bound sites. The N-terminal sequences from RYFRP to NVRAQ are the signal peptide that plays a significant role in expression of FDH.

broad-host-range vector pBBR1-MCS4 [31] inserted with a fragment of a putative promoter region of the *adhAB* gene of *G. oxydans* 621H and a fragment of the complete fdh_{ATG} gene. The site-directed mutation was introduced to the plasmid by replacing one of the TGT and TGC codons corresponding to Cys235 and Cys 238 by the GCC codon (corresponding to Ala). The site-directed mutation Cys235 and Cys 238 were introduced to the *fdh* gene by inverse polymerase chain reaction (PCR) using primers fdhC_heme1*c*KO(+) (5′-TGCCGCGGCCGCCCATACCAATGGGCGTGACGGTCA ATTTCTTGCTGG-3′) and fdhC_heme1*c*KO(−) (5′-TCGGCGGCAATTGCCAGATAATGACCGC -3′)

To prepare the Δ1*c*FDH variant, an in-frame deletion in the *fdh* gene was introduced to the plasmid pSHO13. The N-terminal amino acid sequences from RYFRP to NVRAQ (Fig. 1) are believed to be a signal peptide that relates to the expression of subunit II; hence, it was not deleted. The signal peptide was predicted by SignalP4.1 [32]. All sequences except for a part corresponding to heme 1*c*, were amplified by Herculase II fusion DNA polymerase using primers fdhC_AARIEGK(+) (5′-GCGGCAAGAATCGAAGGCAAACCC-3′) and fdhC_SignalTerminal(−) (5′-TTGCGCCCGTACGTTCGTCCCTGCGAG -3′), and the PCR products were self-ligated. In order to avoid some risks of wrong copies at the vector in inverse PCR, the fragment of complete fdh_{ATG} gene was inserted into pT7Blue (Novagen, Merck, USA), and then the in-frame deletion was introduced. pSHO13 was treated with HindIII and BamHI, and a 3.5 kbp DNA fragment corresponding to most of subunit I and all of subunits II and III was inserted into pT7Blue, which

was treated with HindIII and BamHI, and then performed the avobe-mentioned PCR. All nucleotide sequences of the mutated fdh_{ATG} gene of PCR products were confirmed by Fasmac sequencing service (Japan). The mutated fdh_{ATG} gene was treated with HindIII and BamHI, and a 3.1 kbp DNA fragment was inserted into pSHO13 that was treated with HindIII and BamHI to yield pYUF23 and pYUF27.

G. oxydans NBRC12528 Δ*adh*A::Km^r was transformed with pYUF23 and pYUF27 via a triparental mating method using the HB101 strain that includes pRK2013 [33]. *Gluconobacter* cells were cultivated, and then recombinant (native) FDH and the mutant were purified as described in a previous paper [23] with a little modification as described below. The elution of Δ1*c*FDH from a DEAE-Sepharose column was performed using a concentration gradient of McIlvain buffers (McB) at pH 6.0 from 20-fold-diluted McB to 4-fold-diluted McB that contained 1 mM 2-mercaptoethanol and 0.1% (w/v) Triton X-100 (M = mol dm^{-3}).

Sodium dodecyl sulfate-polyacrylamide gel electrophoresis (SDS-PAGE) was performed on a 12.5% acrylamide gel at 100 V at room temperature, and proteins were stained with Coomassie Brilliant Blue.

Strain	Description	Source or reference
Escherichia coli		
DH5α	F$^-$*endA1hsdR17(r$_k^-$ m$_k^+$) supE44thi-1λ$^-$recA1gyrA96relA1 deoRΔ(lacZYA-argF)U169Φ80dlacZΔM15*	[34]
HB101	F$^-$*thi-1 hsdS20*(r$_B$m$_B$)*supE44recA13ara14leuB6proA2 lacY1galK2rpsL20*(Str^r*xyl-5 mtl-1λ$^-$*)	[35]
Gruconobacter oxydans		
NBRC12528 Δ*adh*A mutant	NBRC12528 Δ*adh*A::Km^r	[36]

Plasmid	Description	Source or reference
pKR2013	Plasmid mediates plasmid transfer; Km^r	[33]
pT7Blue	General purpose cloning vector	Novagen
pBBR1MCS-4	Broad-host-range plasmid; *mob* Ap^r	[31]
pSHO8	pBBR1MCS-4, a 0.7-kb fragment a putative promoter region of the *adhAB* gene of *G*.oxydans621H	[23]
pSHO13	pBBR1MCS-4,a 3.7-kb fragment of the *fdh$_{ATG}$* genes, a 0.7-kb fragment a putative promoter region of the *adhAB* gene of *G*.oxydans621H	[23]

| pYUF23 | pBBR1MCS-4,a 3.7-kb fragment of the *fdh*$_{ATG}$ genes carrying C235A and C238A mutation, a 0.7-kb fragment a putative promoter region of the *adhAB* gene of *G.*oxydans621H | This study |
| pYUF27 | pBBR1MCS-4,a 3.7-kb fragment of the *fdh*$_{ATG}$ genes introduced in-frame deletion, a 0.7-kb fragment a putative promoter region of the *adhAB* gene of *G.*oxydans621H | This study |

Table 1. Bacterial strains and plasmids used in this study

Electrochemical Measurements

  Cyclic voltammetry and chronoamperometry were performed on an ALS 611s voltammetric analyzer under anaerobic conditions. The working electrode was an Au electrode, whereas the reference and counter electrodes included a handmade Ag|AgCl|sat.KCl electrode and a Pt wire, respectively. All potentials are referred to the reference electrode in this paper. Cyclic voltammograms (CAs) were recorded at 25 °C and a scan rate (v) of 10 mV s^{-1} in 1.0 mL of a McB (pH 4.5) that contained 0.1 M D-fructose (L = dm^3). Chronoamperograms (CAs) were recorded under the same conditions. For measurements of the DET-type catalytic waves, a 3 μL aliquot of the corresponding enzyme stock solution was added to the buffer solution. The author fixed the enzyme activity per volume (activity-based enzyme concentration, c_A) at 4×10^2 U mL^{-1} and the concentration of Triton X-100 at 0.1% (w/v) for the enzyme stock solutions used in this work. Here, one unit (U) of the FDH activity is defined as the amount of enzyme oxidizing 1 μmol of D-fructose per minute at pH 4.5.

Oxygen consumption rates by intact cells

  Oxygen consumption rate of whole cells was measured as described in

Other Analytical Methods

  The FDH activity was spectrophotometrically measured with potassium ferricyanide (as an electron acceptor) and the ferric dupanol reagent, as described in the literature [22]. The total protein concentration (c_t) was determined using a DC protein assay kit (Bio-Rad, CA) that used bovine serum albumin as the standard.

Result and Discussion

The author constructed and purified Δ1*c*-siteFDH, then performed SDS-PAGE and stained heme *c* by 3,3',5,5'-tetramethylbenzidine (Fig. 2 (B)). The subunit II of Δ1*c*-siteFDH was not observed at 51 kDa, and a new band was observed at 36 kDa. Hence, the author determined the N-terminal amino acid sequence of the new band at 36 kDa. The sequence was "AARIEGKPYVFDHTHNDDWN" (from N- to C-terminal) and it is founded in Subunit II (Fig.1). This unexpected result indicated that the subunit II of Δ1*c*-siteFDH was probably cut by a protease of *G. oxydans* NBRC 12528 in the soluilization or purification step, and that Δ1*c*-siteFDH loss the sequence involving the binding site of heme 1*c*. In order to construct a stable variant that lacks heme 1*c* moietiy, the author constructed Δ1*c*FDH that lacks the amino acid sequence involving the binding site of heme 1*c* as well as Δ1*c*-siteFDH.
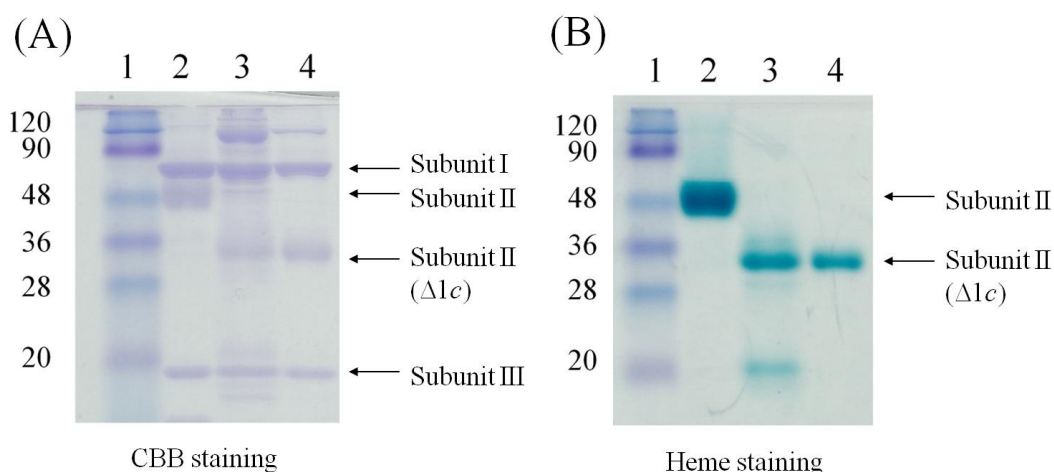
Figure 2. SDS-PAGE photograph of the purified recombinant (native) FDH and variants. heme *c* moieties in Subunit II are stained by (A) CBB and (B) 3,3',5,5'-tetramethylbenzidine. Lane 1, Molecular mass standard (sizes in kDa are shown on the left); Lane 2, recombinant (native) FDH, Lane 3, Δ1*c*-siteFDH, Lane 4, Δ1*c*FDH.

The author constructed and purified Δ1*c*FDH. The SDS-PAGE results indicated that Δ1*c*FDH was acceptably purified, and subunit II was downsized from 51 kDa to 36 kDa (Fig. 2). The evaluated molecular mass of subunit II is close to that expected from the protein engineering procedure. The heme-based enzyme concentration (c_E) of the recombinant (native) FDH was spectrophotometrically determined using the adsorption coefficient of the reduced heme *c* at 550 nm ($\varepsilon_{550\,nm}$ = 23,000 M^{-1} cm^{-1} [37]). c_E of Δ1*c*FDH was evaluated by assuming that the adsorption coefficient of Δ1*c*FDH is two-thirds that of the recombinant (native) FDH, as there are two heme *c*

moieties in $\Delta 1c$FDH and three in the recombinant (native) FDH. c_E determined spectrophotometrically and c_t determined using the DC protein assay kit were 15 μM and 1.7 g L^{-1}, respectively, for the recombinant (native) FDH solution; the values were 28 μM and 10 g L^{-1}, respectively, for the $\Delta 1c$FDH solution. The results indicate that the purity of the $\Delta 1c$FDH solution is lower than that of the recombinant (native) FDH solution; c_E/c_t was 2.8 μmol g^{-1} and 8.8 μmol g^{-1} for $\Delta 1c$FDH and the recombinant (native) FDH, respectively. Because c_A was set at 4×10^5 U L^{-1} for both of the enzyme solutions, the data indicate that the enzyme activity of $\Delta 1c$FDH is approximately one-half that of the recombinant (native) FDH; c_A/c_E was 1.4×10^{10} U mol^{-1} and 2.7×10^{10} U mol^{-1} for $\Delta 1c$FDH and the recombinant (native) FDH, respectively.

Fig. 3(A) shows the cyclic voltammograms (CVs) of the recombinant (native) FDH- and $\Delta 1c$FDH-adsorbed Au electrodes in the presence of D-fructose. A clear DET-type catalytic wave attributed to the D-fructose oxidation was observed at both of the enzyme-adsorbed electrodes. These results indicate that the deleted region does not play a significant role and is not involved in the DET-type bioelectrocatalysis. The waves were not affected by stirring; therefore, the catalytic current is independent of the mass transfer of the substrate, and it is instead controlled by the enzyme kinetics and the interfacial electron transfer kinetics [37-42].

The currents approached a limiting value at positive potentials. However, when the measurements were performed at potentials more positive than 0.5 V, the catalytic currents decreased because of Au oxide layer formation [25, 43]. Therefore, the author utilized the steady-state current density of 0.5 V as a limiting current density (j_{lim}) in this study. The j_{lim} value at the $\Delta 1c$FDH-adsorbed electrode was approximately one and a half times as large as that at the recombinant (native) FDH-adsorbed electrode; j_{lim} was 0.29 (± 0.04) mA cm^{-2} and 0.20 (± 0.03) mA cm^{-2} for $\Delta 1c$FDH and the recombinant (native) FDH, respectively, in three repeated experiments, and $j_{lim,\Delta 1c FDH}/j_{lim,FDH} \cong 1.6$. The j_{lim} value, which is completely controlled by the enzyme kinetics, is given by [37-42]

$$j_{lim} = n_S F k_{cat} \Gamma_{eff}, \tag{1}$$

where n_S is the number of electrons of the substrate, F is the Faraday constant, k_{cat} is the catalytic constant, and Γ_{eff} is the surface concentration of "electrochemically efficient" enzymes. If the author assume that k_{cat} is identical for both $\Delta 1c$FDH and the recombinant (native) FDH, the increase in j_{lim} by the downsizing protein engineering is simply attributable to an increase in Γ_{eff}. If the author assumes that k_{cat} is proportional to c_A/c_E, the mutation inevitably induces a threefold increase in Γ_{eff}.

$$\frac{\Gamma_{\Delta 1c FDH}}{\Gamma_{FDH}} = \frac{j_{lim,\Delta 1c FDH} k_{cat,FDH,}}{j_{lim,FDH} k_{cat,\Delta 1c FDH,}} = \frac{j_{lim,\Delta 1c FDH} (c_A/c_E)_{FDH}}{j_{lim,FDH} (c_A/c_E)_{\Delta 1c FDH}} \cong 2.8.$$

This increase in Γ_{eff} may not be expected simply by the downsizing of subunit II (36 kDa/51 kDa) in light of the total molecular mass of the recombinant (native) FDH (ca. 140 kDa). Therefore, it is considered that the variant adsorbs in an orientation(s) that is more suitable for DET-type
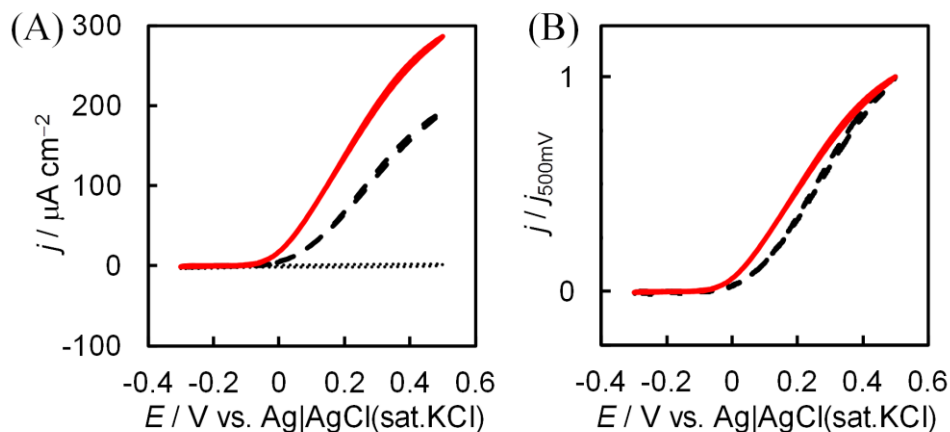
Figure 3. CVs (A) and normalized CVs (B) of D-fructose oxidation at the recombinant (native) FDH- (broken line) or the Δ1cFDH- (solid line) adsorbed electrodes in McB (pH 4.5) in the presence of 100 mM D-fructose under anaerobic conditions. The scan rate was 10 mV s^{-1}. The dotted line indicates the background at the bare Au electrode.

bioelectrocatalysis.

Fig. 3(B) shows the CVs of Fig. 3(A) normalized against the current at 0.5 V. The half-wave potential ($E_{1/2}$) of the steady-state catalytic wave at the Δ1cFDH-adsorbed electrode is 0.05 V more negative that that at the recombinant (native) FDH-adsorbed electrode. Because the onset potential is almost independent of the mutation, the negative shift in $E_{1/2}$ may be attributed to an increase in $k°$. It can be reasonably expected that the deletion of the N-terminus that includes the heme 1c moiety decreases the distance between heme 2c and the electrode surface.

The effects of the protein engineering on the enzyme stability were chronoamperometrically investigated. Fig. 4 shows the CAs, which are normalized against the current at the start of the measurements for the recombinant (native) FDH- or Δ1cFDH- adsorbed Au electrodes at 0.5 V in the presence of D-fructose. The current of the Δ1cFDH-adsorbed electrode decreased slightly faster than that of the recombinant (native) FDH-adsorbed electrode, although after the first one hour the rates of the current decrease were almost identical with each other. The protein engineering may make the enzyme slightly more sensitive to the electrical double layer effect [43] at high potentials, resulting in slight decrease in the tolerance for continuous operation.
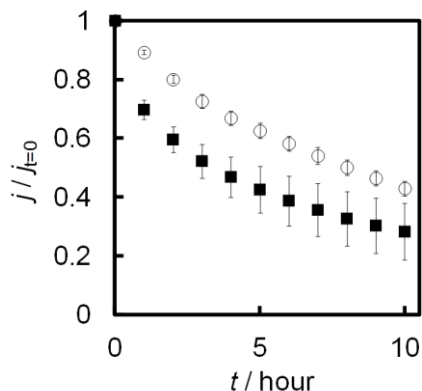
Figure 4. Stability during the continuous operation of the recombinant (native) FDH (open circles) or Δ1cFDH (closed squares) adsorbed on electrodes at 0.5 V in McB (pH 4.5) and in the presence of 100 mM D-fructose under anaerobic conditions. The error bars were evaluated using Student's *t*-distribution at a 90% confidence level in three repeated experiments.

Oxygen consumption rate with D-fructose by the intact cells harboring pSHO13 (recombinant (native) FDH), pYUF27 (Δ1cFDH) and pSHO8 (control: empty vector) was measured (Fig.5). D-fructose dependent oxygen consumption rate by the Δ*adhA* cells harboring empty vector (pSHO8) was much lower than oxygen consumption with glucose by the same cells. This result suggests that the Δ*adhA* strain and even the parental strain *G. oxydans* NBRC12528 have the glucose oxidizing respiration chain as previously reported [44], but they do not have fructose oxidizing respiration chain. The Δ*adhA* cells harboring recombinant (native) FDH expression vector (pSHO13) show the ability to consume oxygen depending on D-fructose about one and half times faster than that with glucose. However, the Δ*adhA* cells harboring Δ1cFDH expression vector (pYUF27) do not have D-fructose oxidizing respiration chain. This result suggests that the heme 1*c* moiety is involved in *in vivo* electron transfer systems. In addition, the electron transfer pathway in *in vivo* catalytic reaction is different from that in DET-type bioelectrocatalysis. Because the distance between the active site and an electrode surface is important in DET-type bioelectrocatalysis, the electrons transfer pathway is different from that in *in vivo* enzymatic catalytic reaction.
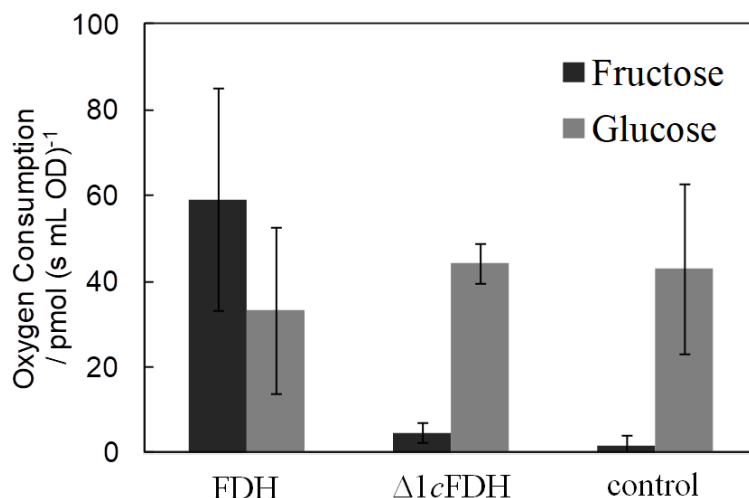
Figure 5. D-Fructose-dependent oxygen consumption (heavy gray columns) of the intact cell preparations of the *ΔadhA* strains harboring pSHO13 (recombinant (native) FDH), pYUF27 (Δ1*c*FDH) and pSHO8 (control). Control experiments were also conducted with D-glucose (light gray columns). The rates of oxygen consumption were normalized by optical density of the cell preparations. Data are shown as mean values with 90% confidence intervals (error bars; *n*=3).

Conclusion

The author successfully constructed a variant of Δ1*c*FDH that lacks the N-terminus 143 amino acid residues including heme 1*c*. The Δ1*c*FDH variant that was adsorbed on an Au electrode produced a large DET-type bioelectrocatalytic wave for D-fructose oxidation. The results clearly support our previous conclusion that the electrons accepted at the FAD in subunit I are transferred to electrodes via heme 3*c* and heme 2*c* in subunit II without going through heme 1*c*. Heme 1*c* may be located somewhat far from the other heme *c* moieties. The DET-type bioelectrocatalytic activity increased approximately one and a half times, although the solution activity decreased to one-half of the recombinant (native) FDH. A negative shift in $E_{1/2}$ was also observed. Downsizing the protein engineering resulted in an increase in Γ_{eff} (due to an increase in the population of the electrochemically suitable orientation and an increase in the total surface concentration) and improved the interfacial electron transfer kinetics. The variant Δ1*c*FDH is useful for construction of DET-type bioelectrochemical devices such as biofuel cells and biosensors. The strategy of the deletion of such a long region that includes one of the prosthetic groups taking the electron transfer pathway in consideration is useful for improving the properties of the DET-type bioelectrocatalysis of other redox enzymes.

References

[1]   S.V. Hexter, T.F. Esterle, F.A. Armstrong, A unified model for surface electrocatalysis based on observations with enzymes, Phys. Chem. Chem. Phys. 16 (2014) 11822

[2]   C. Léger, P. Bertrand, Direct electrochemistry of redox enzymes as a tool for mechanistic studies, Chem. Rev. 108 (2008) 2379.

[3]   M.J. Moehlenbrock, S.D. Minteer, Extended life time biofuel cells, Chem. Soc. Rev. 37 (2008) 1188.

[4]   N. Mano, F. Mao, A. Heller, A miniature membrane-less biofuel cell operating at +0.60 V under physiological conditions, ChemBioChem. 5 (2004) 1703.

[5]   D. Leech, P. Kavanagh, W. Schuhmann, Enzymatic fuel cells: recent progress, Electrochim. Acta. 84 (2012) 223.

[6]   S.C. Barton, J. Gallaway, P. Atanassov, Enzymatic biofuel cells for implantable and microscale devices, Chem. Rev. 104 (2004) 4867.

[7]   S. Shleev, J. Tkac, A. Christenson, T. Ruzgas, A.I. Yaropolov, J.W. Whittaker, L. Gorton, Cellobiose dehydrogenase modified electrodes: advances by materials science and biochemical engineering, Anal. Bioanal. Chem. 405 (2013) 3637.

[8]   N. Mano, L. Edembe, Bilirubin oxidases in bioelectrochemistry: Features and recent findings, Biosens. Bioelectron. 50 (2013) 478

[9]   V. Fourmond, C. Léger, Modeling the voltammetry of adsorbed enzymes and molecular catalysts, Curr. Opin. Electrochem.(2017) t110

[10]   W. Zhang, G. Li, Third-generation biosensors based on the direct electron transfer of proteins, Anal. Aci. 20 (2004) 603.

[11]   T. Ikeda, Bioelectrochemical studies based on enzyme-electrocatalysis, Electrochim. Acta. 82 (2012) 158.

[12]   D. Ratautas, A. Laurynėnas, M. Dagys, L. Marcinkevičiencė, R. Meškeys, J. Kulys, High current, low redox potential mediatorless bioanode based on gold nanoparticles and glucose dehydrogenase from *Ewingella americana*, Electrochim. Acta 199 (2016) 254.

[13]   M. Dagys, K. Haberska, S. Shleev, T. Arnebrant, J. Kulys, T. Ruzgas, Laccase-gold nanoparticle assisted bioelectrocatalytic reduction of oxygen, Electrochem. Commun. 12 (2010) 933.

[14]   A.A. Karyakin, Principles of direct (mediator free) bioelectrocatalysis, Bioelectrochemistry 88 (2012) 70.

[15]   T. Ikeda, F. Matsushita, M. Senda, Amperometroc fructose sensor based on direct bioelectrocatalysis, Biosens. Bioelectron. 6 (1991) 299.

[16]   Y. Kamitaka, S. Tsujimura, N. Setoyama, T. Kajino, K. Kano, Fructose/dioxygen biofuel cell based on direct electron transfer-type bioelectrocatalysis, Phys. Chem. Chem. Phys. 9 (2007)

1793.

[17]   Y. Kamitaka, S. Tsujimura, K. Kano, High current density bioelectrolysis of D-fructose at fructose dehydrogenase-adsorbed and ketjen black-modified electrodes without a mediator, Chem. Lett. 36 (2007) 218.

[18]   H. Xia, Y. Hibino, Y. kitazumi, O. Shirai, K. Kano, Interaction between d-fructose hydrogenase and mthoxy-substituted-functionalized carbon surface to increase productive orientations, Electrochim. Acta. 218 (2016) 41.

[19]   R. Antiochia, L. Gorton, A new osmium-polymer modified screen-printed graphene electrode for fructose detection, Sens. Actuators B 195 (2014) 287.

[20]   K. Nakashima, H. Takei, O. Adashi, E. Shinagawa, M. Ameyama, Determination of seminal fructose using D-fructose dehydrogenase, Clin. Chim. Acta 151 (1985) 307.

[21]   K. So, S. Kawai, Y. Hamano, Y. Kitazumi, O. Shirai, M. Hibi, J. Ogawa, K. Kano, Improvement of a direct electron transfer-type fructose/dioxygen biofuel cell with a substrate-modified miocathode, Phys. Chem. Chem. Phys., 16 (2014) 4823.

[22]   M. Ameyama, E. Shinagawa, K. Matsushita, O. Adachi, D-Fructose dehydrogenase of *gluconobacter industrius*: purification, characterization, and application to enzymatic microdetermination of D-fructose, J. Bacteriol. 145 (1981) 814.

[23]   S. Kawai, M. Tsutsumi, T. Yakushi, K. Kano, K. Matsushita, Heterologous overexpression and characterization of a flavoprotein-cytochrome *c* complex fructose dehydrogenase of *gluconobacter iapinicus* NBRC3260, Appl. Environ. Microbiol. 79 (2013) 1654.

[24]   S. Kawai, T. Yakushi, K. Matsushita, Y. Kitazumi, O. Shirai, K. Kano, The electron transfer pathway in direct electrochemical communication of fructose dehydrogenase with electrodes, *Electrochem. Commun,* 38 (2014) 28.

[25]   Y. Hibino, S. Kawai, Y. Kitazumi, O. Shirai, K. Kano, Electrochem. Commun., 67 (2016) 43.

[26]   R.A. Marcus, Electron transfer reactions in chemistry: theory and experiment, Angew. Chem. Int. Ed. 32 (1993) 1111.

[27]   K. Kataoka, H. Komori, Y. Ueki, Y. Konno, Y. Kamitaka, S. Kurose, S. Tsujimura, Y. Higuchi, K. Kano, D. Seo, T. Sakurai, Structure and function of the engineered multicopper oxidase CueO from *Escherichia coli* –Deletion of the methionine-rich helical region covering the substrate-binding site, J. Mol. Biol. 373 (2007) 141.

[28]   G. Presnova, V. Grigorenko, A. Egorov, T. Ruzgas, A. Lindgren, L. Gorton, T. Börchers, Direct electron transfer of recombinant horseradish peroxidase on gold, Faraday Discus. 116 (2000) 281

[29]   O. Courjean, F. Gao, N. Mano, Deglycosylation of glucose oxidase for direct and efficient glucose electrooxidation on a glassy carbon electrode, Angw. Chem., Int. Ed. 48 (2009) 5897

[30]   R. Ortiz, H. Matsumura, F. Tasca, K. Zahma, M. Samejima, K. Igarashi, R. Ludwig, L.

Gorton, Effect of deglycosylation of cellobiose dehydrogenase on the enhancement of direct electron transfer with electrodes, Anal. Chem. 84 (2012)10315.

[31]   M.E. Kovach, P.H. Elzer, D.S. Hill, G.T. Robertson, M.A. Farris, R.M. Roop, K.M. Peterson, Four new derivatives of the broad-host-range cloning vector pBBR1MCS, carrying different antibiotic-resistance cassettes, Gene 166 (1995) 175.

[32]   T.N. Petersen, S. Brunak, G. von Heijne, H. Nielsen, SignalP 4.0: discriminating signal peptides from transmembrane regions, Nat. Methods 8 (2011) 785.

[33]   D.H. Figurski, D.R. Helinski, Replication of an origin-containing derivative of plasmid RK2 dependent on a plasmid function provided in trans, Proc. Natl. Acad. Sci. U. S. A. 76 (1979) 1648.

[34]   S.G. Grant, J. Jessee, F.R. Bloom, D. Hanahan, Differential plasmid rescue from transgenic mouse DNAs into *Escherichia coli* methylationrestriction-mutants, *Proc. Natl. Acad. Sci. U. S. A.,* 87 (1990) 4645

[35]   H.W. Boyer, D. Roulland-Dussoix, A complementation analysis of the restriction and modification of DNA in *Escherichia coli,. J. Mol. Biol.,* 41 (1969) 459

[36]   H. Habe, Y. Shimada, T. Yakushi, H. Hattori, Y. Ano, T. Fukuoka, D. Kitamoto, M. Itagaki, K. Watanabe, H. Yanagishita, K. Matsushita, K. Sakaki, Microbial production of glyceric acid, an organic acid that can be mass produced from glycerol, *Appl. Environ. Microbiol.,* 75 (2009) 7760

[37]   J. Marcinkeviciene, G. Johansson, Kinetic studies of the active sites functioning in the quinohemoprotein fructose dehydrogenase, FEBS Lett. 318 (1993) 23-26.

[38]   C. Léger, A.K. Jones, S.P.J. Albracht, F.A. Armstrong, Effect of a dispersion of interfacial electron transfer rates on steady state catalytic electron transport in [NiFe]-hydrogenase and other enzymes, J. Phys. Chem. B 106 (2002) 13058.

[39]   C. Léger, A.K. Jones, W. Roseboom, S.P.J. Albracht, F.A. Armstrong, Enzyme electrokinetics: hydrogen evolution and oxidation by *allochromatium vinosum* [NiFe]-hydrogenase, Biochemistry 41 (2002) 15736.

[40]   Y. Sugimoto, Y. Kitazumi, O. Shirai, K. Kano, Role of 2-mercaptoethanol in direct electron transfer-type bioelectrocatalysis of fructose dehydrogenase at Au electrodes, Electrochim. Acta 170 (2015) 242.

[41]   H. Xia, Y. Kitazumi, O. Shirai, K. Kano, Enhanced direct electron transfer-type bioelectrocatalysis of bilirubin oxidase on negatively charged aromatic compound-modified carbon electrode, J. Electroanal. Chem. 763 (2016) 104.

[42]   K. So, Y. Kitazumi, O. Shirai, K. Kano, Analysis of factors governing direct electron transfer-type bioelectrocatalysis of bilirubin oxidase at midified electrodes, J. Electroanal. Chem. 783 (2016) 316.

[43]   Y. Sugimoto, Y. Kitazumi, O. Shirai, K. Kano, Role of 2-mercaptoethanol in direct electron transfer-type bioelectrocatalysis of fructose dehydrogenase at Au electrodes, Electrochim. Acta 170 (2015) 242.

[44]   K. Matsushita, E. Shinagawa, O. Adachi and M. Ameyama, Reactivity with ubiquinone of quinoprotein D-glucose dehydrogenase from *Gluconobacter suboxydans, J. Biochem.*, 105 (1989) 633.

Chapter3

Protein-Engineering Improvement of Direct Electron Transfer-Type Bioelectrocatalytic Properties of D-Fructose Dehydrogenase

D-Fructose dehydrogenase (FDH) contains a flavin adenine dinucleotide (FAD) in subunit I and three heme c moieties ($1c$, $2c$, and $3c$ from the N-terminus) as the electron transfer relaying sites. The electron transfer in direct electron transfer-type bioelectrocatalysis of FDH is proposed to proceed in sequence from FAD, through heme $3c$, to heme $2c$ without going through heme $1c$. In order to improve the performance of the bioelectrocatalysis, the author constructed a variant (M450QΔ1cFDH). M450QΔ1cFDH lacks 143 amino acid residues involving heme $1c$ and its amino acid residue M450 as the sixth axial ligand of heme $2c$ was replaced with glutamine to negatively shift the formal potential of heme $2c$. M450QΔ1cFDH was adsorbed on a planar gold electrode. The variant-adsorbed electrode produced a clear sigmoidal steady-state catalytic wave of fructose oxidation in cyclic voltammetry. The limiting current density was 1.4 times larger than that of recombinant (native) FDH. Additionally, the half-wave potential of the wave was shifted by 0.2 V to the negative direction. M450QΔ1cFDH adsorbed rather homogeneously in orientations suitable for DET-type bioelectrocatalysis.

Introduction

Direct electron transfer- (DET-) type bioelectrocatalysis is a coupled reaction of a redox enzymatic reaction and an electrode reaction without mediators [1-11]. DET-type bioelectrocatalysis is attracting significant attention for construction of mediatorless biosensors and biofuel cells and for fundamental analysis of redox properties of enzymes [12, 13]. In DET-type bioelectrocatalysis, the redox active site in the adsorbed enzyme directly communicates with electrodes. However, there is a limit to the number of enzymes that show clear DET-type catalytic activity, since the redox active sites are in many cases embedded in the insulating peptide of the enzyme [14].

The author's group has been focusing on D-fructose dehydrogenase (FDH) from *Gluconobacter japonicus* NBRC 3260 as a model enzyme of DET-type bioelectrocatalysis [15, 16]. FDH is a membrane-bound enzyme that produces DET-type catalytic wave of fructose oxidation in large current densities [17-19]. A biofuel cell with DET-type bioelectrocatalysis using FDH on the anode exhibited a high power density (2.6 mW cm^{-2} under quiescent conditions) [20]. FDH is a heterotrimeric enzyme complex that consists of subunits I (67 kDa), II (51k Da), and III (20 kDa) [21]. Subunit I has one covalently bound flavin adenine dinucleotide (FAD) at which D-fructose is oxidized. Subunit II has three heme c moieties as the electron transfer relaying sites: heme $1c$ with M301 as the sixth axial ligand, heme $2c$ with M450, and heme $3c$ with M578 from the N-terminus.

The electron transfer in the DET reaction of FDH is proposed to proceed in sequence from the FAD, through heme $3c$, to heme $2c$ (as the electron-donating site to electrodes) without going through heme $1c$ [23, 24] (Fig. 1(A)). Subunit III plays a key role in the expression of FDH [22-25].

For improvement of the DET-type bioelectrocatalysis, several enzyme modification approaches were attempted [26]: (i) trimming of the N- or C-terminals and deglycosylation to reduce the size of enzymes and to open up the redox active site [27-30], (ii) site-directed mutagenesis at the redox active site to change its redox and catalytic characteristics[31, 32], and (iii) addition of the tag sequences to control the orientation of enzymes [28, 33].

In this study, the author attempted to take two strategies in order to improve the performance of the DET-type bioelectrocatalysis of FDH: (a) trimming of the N-terminal to reduce the enzyme size and (b) site-directed mutation to decrease the overpotential. For this purpose, the author designed a variant M450QΔ1cFDH in which 143 amino acid residues involving heme $1c$ were removed, and M450 as the sixth axial ligand of heme $2c$ was replaced with glutamine to shift the formal potential of heme $2c$ to the negative potential side. As a result, M450QΔ1cFDH-adsorbed electrode exhibited high current density and small overpotential compared to the recombinant (native) FDH-adsorbed electrode in DET-type bioelectrocatalysis. The author also discuss conceivable electrostatic interaction between M450QΔ1cFDH and charged electrode surface.

All variants were adsorbed on a planar gold electrode and DET-type catalytic currents were measured by linear sweep voltammetry. Detailed analysis of the steady-state catalytic current was performed.
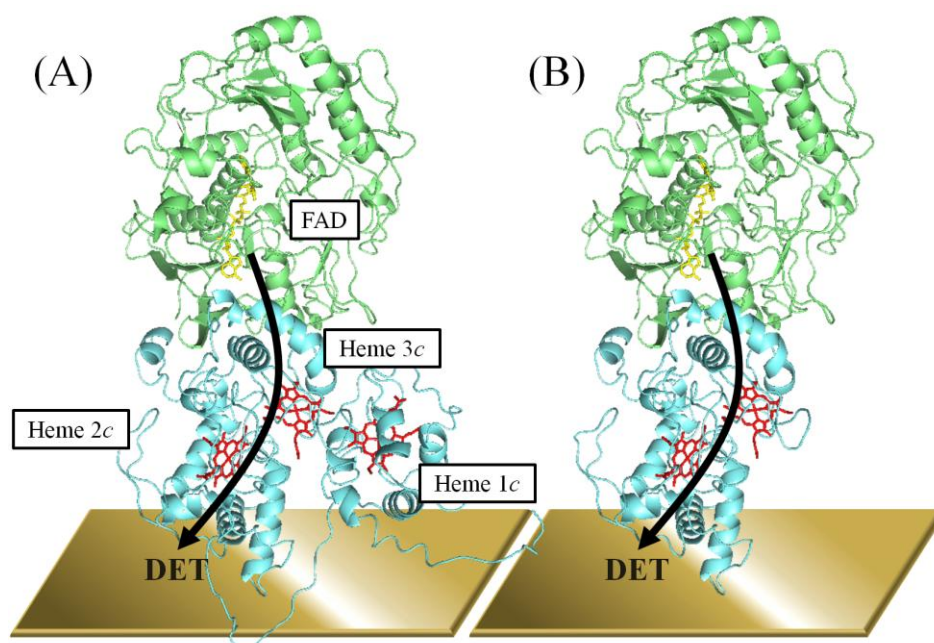
Figure 1. Schematic of orientations suitable for DET-reaction of (A) FDH and (B) M450QΔ1*c*FDH-variant based on homology modeling. Structural data of FAD-glucose dehydrogenase from *Aspergillus flavus* (PDB 4YNT) and thiosulfate dehydrogenase from *Marichromatium purpuratum* "isolated" (PDB 5LO9) were used as templates of subunits I (green) and II (blue), respectively, in the homology modeling. The small subunit III was not considered in the modeling for lack of structural information of similar enzymes.

Experimental

Materials

Herculase II fusion DNA polymerase and restriction endonucleases were purchased from Agilent Technologies (Santa Clara, CA) and Takara Shuzo (Japan), respectively. DNA ligase was obtained from Toyobo (Japan). Potassium ferricyanide was obtained from Nakalai Tesque (Japan). Other chemicals were obtained from Wako Pure Chemical Industries (Japan).

Preparation of the mutants and FDH

To prepare the M450QΔ1cFDH variant, two mutations were introduced to the *fdh* gene of the plasmid pSHO13 that was used for expressing the recombinant (native) FDH [22]. pSHO13 is a broad-host-range vector pBBR1-MCS4 [34] inserted with a fragment of a putative promoter region of the *adhAB* gene of *G. oxydans* 621H and a fragment of the complete *fdh*$_{ATG}$ gene. The site-directed mutation M450Q was introduced to the *fdh* gene by inverse polymerase chain reaction (PCR) using primers fdhC_heme2cGln(+) (5′-ACAGGCAGAAGCAATCGAGCATAGCC-3′) and fdhC_heme2c(−) (5′-GGTCCTGCTGCACGAGCATGTG-3′). An in-frame deletion of the region containing the heme 1c moiety was introduced by PCR using primers fdhC_AARIEGK(+) (5´-GCG GCAAGAATCGAAGGCAAACCC-3´) and fdhC_SignalTerminal(−) (5´-TTGCGCCCGTACGTTC GTCCCTGCGAG-3´). In order to avoid some risks of wrong copies at the vector in inverse PCR, the fragment of complete *fdh*$_{ATG}$ gene was inserted into pT7Blue, and then inverse PCR was performed. All nucleotide sequences of the mutated *fdh*$_{ATG}$ gene of the PCR products were confirmed by Fasmac Sequencing Service (Japan). Then the fragment of mutated *fdh*$_{ATG}$ gene was inserted into pSHO8 in order to yield pYUF29. pYUF29 was used for expression of M450QΔ1cFDH variant.

G. oxydans NBRC 12528 Δ*adhA*::Km^r was transformed with pYUF29, as described in a previous paper [35]. *Gluconobacter* cells were cultivated, and then the recombinant (native) FDH, M450QΔ1cFDH as well as M450QFDH (a variant with glutamine in place of methionine of the sixth axial ligand of heme 2c) and Δ1cFDH (a variant lacking 143 amino acid residues from the N-terminus) were purified as described in previous papers [22, 25] with some little modifications as described below. All enzymes were solubilized only for 1 h at 4 °C. The elution of Δ1cFDH and M450QΔ1cFDH from a DEAE-sepharose column was carried out using a concentration gradient of McIlvain buffers (McB) at pH 6.0 from 20-fold-diluted McB to 5-fold-diluted McB containing 1 mM 2-mercaptoethanol and 0.1% (w/v) TritonX-100 (M = mol dm^{-3}).

Since the crystal structure of FDH remains unknown, homology modeling was done using the crystal structural data of already characterized FAD-glucose dehydrogenase from *Aspergillus flavus* (PDB 4YNT) for subunit I and thiosulfate dehydrogenase from *Marichromatium purpuratum* "isolated" (PDB 5LO9) for subunit II were used as templates, as described in a previous paper [19].

Multiple alignments were performed by SWISS-MODEL (https://swissmodel.expasy.org). Homology models are constructed by MODELLER (https://salilab.org/modeller). Docking simulations were performed by ZDOCK SERVER (http://zdock.umassmed.edu) under the condition compatible with previous research. This crystal structure model does not have CHR because the template protein does not have CHR. However, CHR seems not to play significant role in DET-type bioelectrocatalysis, because ΔchrFDH (lacking CHR) show clear DET-type catalytic wave according to previous research.

strain	Description	Source or reference
Escherichia coli		
DH5α	F⁻ *endA1hsdR17(rₖ⁻mₖ⁺) supE44thi-1λ⁻recAlgyrA96relA1 deoRΔ(lacZYA-argF)*U169Φ80d*lacZ*ΔM15	[36]
HB101	F⁻ *thi-1 hsdS20*(r_Bm_B)*supE44recA13ara14leuB6proA2 lacY1galK2rpsL20*(Str^r*xyl-5 mtl-1λ⁻)	[37]
Gruconobacter oxydans		
NBRC12528 ΔadhA mutant	NBRC12528 Δ*adh*A::Km^r	[38]

Plasmid	Description	Source or reference
pKR2013	Plasmid mediates plasmid transfer; Km^r	[35]
pT7Blue	General purpose cloning vector	Novagen
pBBR1MCS-4	Broad-host-range plasmid; *mob* Ap^r	[34]
pSHO13	pBBR1MCS-4,a 3.7-kb fragment of the *fdh_ATG* genes, a 0.7-kb fragment a putative promoter region of the *adhAB* gene of *G.*oxydans621H	[22]
pYUF29	pBBR1MCS-4,a 3.7-kb fragment of the *fdh_ATG* genes carrying M450Q mutation introduced in-frame deletion of 143 amino acids involving the heme 1*c* moiety, a 0.7-kb fragment a putative promoter region of the *adhAB* gene of *G.*oxydans621H	This study

Table 1. Bacterial strains and plasmids used in this study

Electrochemical measurements

Cyclic voltammetry and linear sweep voltammetry were performed on an ALS 611s voltammetric analyzer under anaerobic conditions. Polycrystalline Au electrodes were used as the working electrodes. The Au electrode was polished to a mirror-like finish with Al_2O_3 powder (0.02 μm particle size), rinsed with distilled water, and sonicated in distilled water. The reference and counter electrodes were a handmade Ag|AgCl|sat.KCl electrode and Pt wire, respectively. All potentials are referred to the reference electrode in this paper. Cyclic voltammograms (CVs) were recorded at 25 °C at a scan rate (v) of 10 mV s^{-1} in 1.0 mL of McB (pH 4.5) that contained 0.2 M D-fructose (L = dm^3). For measurements of DET-type catalytic waves, a 3 μL aliquot of the enzyme solution was added to the buffer solution. As a result, the electrolysis solution contained 6 μM 2-mercaptoethanol and 3 ppm (w/v) TritonX-100.

Other analytical methods

The FDH activity was spectrophotometrically measured with potassium ferricyanide (as an electron acceptor) and the ferric dupanol regent, as described in the literature [21].

Sodium dodecyl sulfate-polyacrylamide gel electrophoresis (SDS-PAGE) was performed using 12.5% acrylamide gel at 100 V at room temperature, and then heme *c* was stained by 3,3',5,5'-tetramethylbenzidine.

Results and discussion

The M450QΔ1*c*FDH were successfully constructed. The concentrations of the recombinant (native) FDH and variants were spectrophotometrically determined using the absorption coefficient of the reduced heme *c* at 550 nm ($\varepsilon_{550\,nm}$=23,000 M^{-1} cm^{-1}) [39]. The concentration of Δ1*c*FDH, M450QΔ1*c*FDH and were determined considering that Δ1*c*FDH and M450QΔ1*c*FDH have two heme *c* moieties, while recombinant (native) FDH has three heme *c* moieties. Before the electrochemical measurements, all enzyme solutions were diluted with a 50 mM phosphate buffer containing 1 mM 2-mercaptoethanol and 0.1% (w/v) TritonX-100, and the concentrations of the enzymes were adjusted to that of M450QΔ1*c*FDH (7.7 μM). The enzyme activity was evaluated as follows: 2.0×10^{10} U mol^{-1} for the recombinant (native) FDH, 1.8×10^{10} U mol^{-1} for M450QFDH, 1.2×10^{10} U mol^{-1} for Δ1*c*FDH and 1.3×10^{10} U mol^{-1} for M450QΔ1*c*FDH.

Characterizations of the recombinant (native) FDH- and variant-adsorbed electrodes were performed by linear sweep voltammetry in the presence of D-fructose. Each of the enzymes was physically adsorbed on a bare Au electrode. Clear DET-type catalytic waves corresponding to D-fructose oxidation were observed at all of the enzymes-adsorbed electrodes. The current-potential curves were not affected by stirring (Fig. 2). Therefore, the catalytic currents are controlled by the enzyme kinetics and the interfacial electron transfer [40-44].
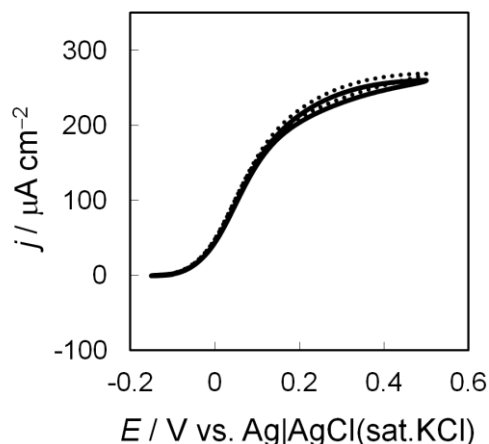
Figure 2. (A): CVs D-fructose oxidation at M450QΔ1*c*FDH-adsorbed Au electrodes in McB (pH4.5) in the presence of 0.2 M D-fructose under anaerobic conditions at v = 10 mV s^{-1} in quiet solution (black solid line) and under convective conditions at ω = 2000 rpm (black dotted line).

In order to characterize the variants, it is important to compare the limiting catalytic current density (j_{lim}) independent of the electrode potential at sufficiently positive potentials. However, measurements at positive potentials more than 0.5 V cause a decrease in the catalytic currents due to a formation of Au oxide layer [24, 42]. Therefore the author measured the steady-state catalytic current density at 0.5 V and used it as j_{lim} in this study. Additionally, the author defined the apparent half-wave potential ($E_{1/2}$) of the catalytic wave as the potential to satisfy $j = j_{\text{lim}}$ /2.

Fig. 3 shows the linear sweep voltammograms (LSV) of the recombinant (native) FDH- and variant (M450QΔ1*c*FDH, M450QFDH and Δ1*c*FDH)-adsorbed electrodes in the presence of D-fructose. $E_{1/2}$ in the M450QFDH-adsorbed electrode was shifted by approximately 0.18 V in the negative direction from that in the recombinant (native) FDH-adsorbed electrode. The j_{lim} value at the Δ1*c*FDH-adsorbed electrode was about 1.6 times higher than that at the recombinant (native) FDH-adsorbed electrode; j_{lim} values were 0.31 ± 0.01 mA cm^{-2} and 0.20 ± 0.01 mA cm^{-2} for Δ1*c*FDH and the recombinant (native) FDH, respectively, in three repeated experiments. It is considered that the negative direction shift of $E_{1/2}$ is attributed to a negative direction shift of the redox potential of the electron-donating site, and that the increased current density is attributed to an increase in the surface concentration of the enzymes on the electrodes [24, 25].
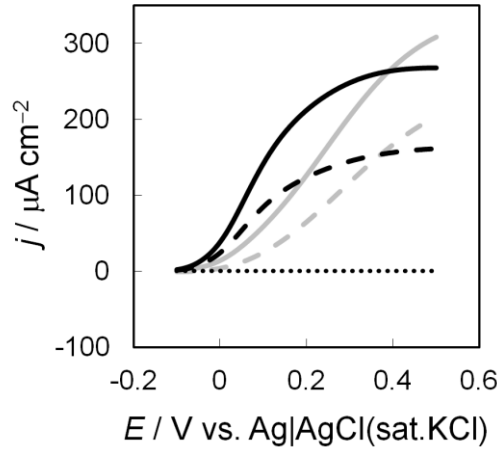
Figure 3. Linear sweep voltammogram of D-fructose oxidation at the recombinant (native) FDH- (dashed gray line), M450QFDH- (dashed black line), $\Delta 1c$FDH- (gray line) and M450Q$\Delta 1c$FDH- (black line) adsorbed electrodes in McB (pH4.5) in the presence of 0.2 M D-fructose under anaerobic conditions. The scan rate was 10 mV s^{-1}. The dotted line indicates the background at the bare Au electrode.

The M450Q$\Delta 1c$FDH-adsorbed electrode exhibited both of the effects of the mutations. $E_{1/2}$ in the M450Q$\Delta 1c$FDH-adsorbed electrode was shifted by approximately 0.20 V in the negative direction from that in the recombinant (native) FDH-adsorbed electrode. Moreover, j_{lim} in the M450Q$\Delta 1c$FDH-adsorbed electrode (0.27 ± 0.01 mA cm^{-2}) was about 1.4 times higher than that in the recombinant (native) FDH-adsorbed electrode. In contrast, the solution activity of M450Q$\Delta 1c$FDH (1.3×10^{10} U mol^{-1}) measured with [Fe(CN)$_6$]$^{3-}$ as an electron acceptor was smaller than that of the recombinant (native) FDH (2.0×10^{10} U mol^{-1}).

Originally, electrode potential- and scan rate (or convection)-independent j_{lim} should be completely controlled by the enzyme kinetics and is given by: [40-45]

$$j_{lim} = n_s F k_{cat} \Gamma_{eff} \qquad (1)$$

where n_s is the number of electrons of the substrate, F is the Faraday constant, k_{cat} is the catalytic constant, and Γ_{eff} is the surface concentration of "electrochemically efficient" enzymes. k_{cat} in Eq. (1) is different from the solution activity that depends on electron acceptors. However, the author may assume that k_{cat} is proportional to the solution activity of a given electron acceptor. On the assumption, it is expected that the increase in j_{lim} of M450Q$\Delta 1c$FDH is attributed to an increase of Γ_{eff} corresponding due to the downsizing protein engineering of the enzyme:

$$\frac{\Gamma_{M450Q\Delta 1c FDH}}{\Gamma_{FDH}} = \frac{j_{lim,M450Q\Delta 1c FDH}}{j_{lim,FDH}} / \frac{k_{cat,M450Q\Delta 1c FDH}}{k_{cat,FDH}} \approx 1.4/0.65 \cong 2.2$$

The M450QFDH- and M450QΔ1*c*FDH-adsorbed electrodes exhibited clear sigmoidal shape in the steady-state catalytic waves; the catalytic currents of the M450QFDH- and M450QΔ1*c*FDH-adsorbed electrodes reached the limiting value at potentials as negative as 0.4 V. The characteristics are in strong contrast with the catalytic waves of the recombinant (native) FDH- and Δ1*c*FDH-electrodes; the catalytic waves increased almost linearly with the electrode potential. The increase is called "residual slope" and is caused by the random orientation of the enzymes adsorbed on an electrode surface [2, 40, 41]. Therefore, it is concluded that M450QFDH and M450QΔ1*c*FDH rather homogeneously adsorbed on the Au electrode in orientations convenient for the DET-type bioelectrocatalysis.

The author assumed orientations most suitable for DET-reaction of recombinant (native) FDH and M450QΔ1*c*FDH, respectively, as shown in Fig. 1. In proposed orientations, the author considered facing subunit II to the electrode surface and locating heme 2*c* in a vertical angle to the electrode, by considering that FDH is a membrane-bound enzyme. As judged from the proposed orientations and structures of FDH and M450QΔ1*c*FDH, it can be expected that the downsizing protein engineering of the enzyme leads to a decrease in the occupied area of the adsorbed enzyme and an increase in the compactness in the (homogeneous) orientation. In addition, the random orientation of recombinant (native) FDH leads to a decrease in Γ_{eff} of the effective enzyme on the electrode, and to an underestimation of j_{lim}, because clear limiting current was not recorded for the recombinant (native) FDH in the potential range investigated. All these factors seem to be able to explain the factor of 2.2 in Eq. (2).

Here the author may point out some singular behaviors of the M450QΔ1*c*FDH variant in DET-type bioelectrocatalytic reaction. When the variant was adsorbed at open circuit potential and the electrode potential was scanned from −0.3 V to 0.5 V, the catalytic wave in the forward positive-going scan was smaller than that in the backward negative-going scan in the first cycle (Fig. 4(A)): during the potential scan, the orientation of the variant seems to be improved at positive potential region. Such hysteresis characteristics were weakened in the second cycle. When the electrode potential was scanned from −0.1 V to 0.5 V, only weak hysteresis characteristics were observed in the first cycle, but not in the second cycle (Fig. 4(B)). Similar characteristics were also observed for the M450Q variant, but not for the recombinant (native) FDH and Δ1*c*FDH. Therefore, the author considered that such hysteresis characteristics were due to some electrostatic interaction between the electrode and the variants with M450Q (variants of which M450 as the sixth axial ligand of heme 2*c* was replaced with glutamine): the variants with M450Q stably and homogeneously adsorb at positively charged electrode surface, but some electrostatic repulsion may occur at negative potentials.

In order to verify our hypothesis, additional experiments were done. When M450QΔ1*c*FDH was adsorbed at 0.5 V, clear steady-state sigmoidal waves were observed without

any hysteresis in the scan from −0.1 V (Fig. 4C). In contrast, when the M450QΔ1*c*FDH-adsorbed electrode was hold at −0.3 V for 3 min and transferred to a fresh electrolysis solution containing D-fructose, the catalytic wave decreased drastically (Fig. 4D), most probably due to the desorption of the variant from the negatively charged electrode surface. Such change in the catalytic wave was observed at M450QFDH-adsorbed electrode, but not at the recombinant (native) FDH- and Δ1*c*FDH-adsorbed electrode: the catalytic wave of the recombinant (native) FDH- and Δ1*c*FDH-adsorbed electrode remained almost unchanged after holding at −0.3 V and transferring to a fresh electrolysis solution.
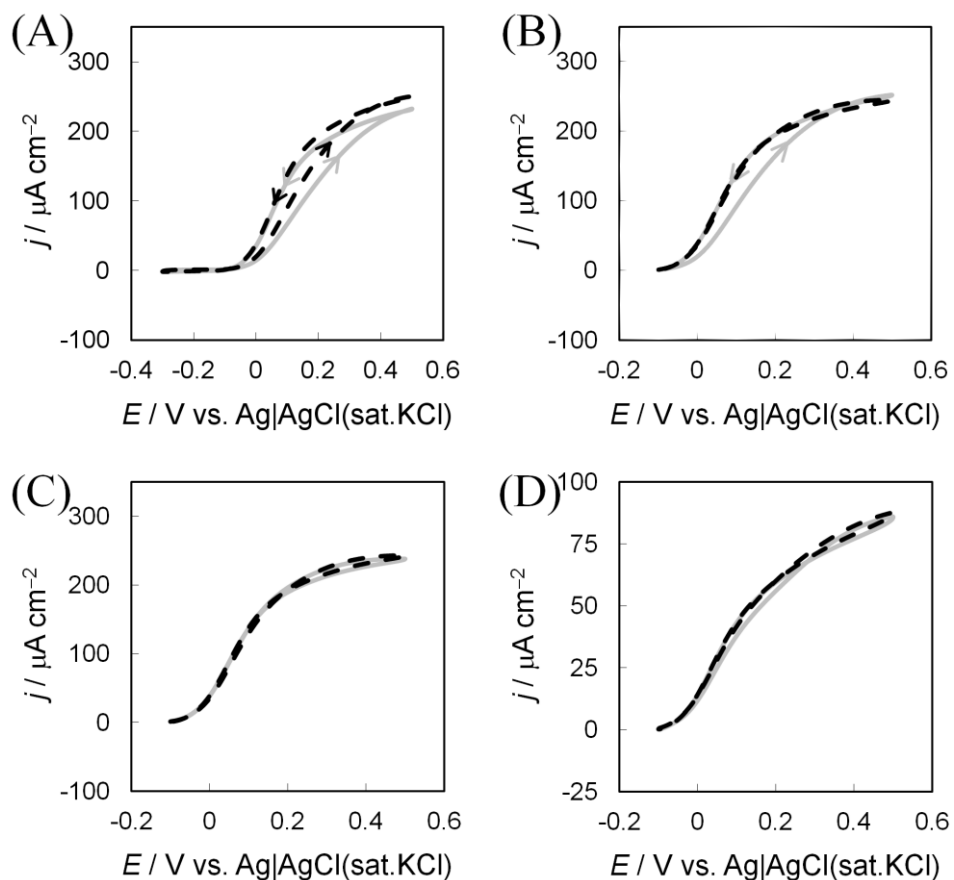
Figure 4. CVs of D-fructose oxidation at M450QΔ1cFDH-adsorbed Au electrodes in McB (pH4.5) in the presence of 0.2 M D-fructose under anaerobic conditions at $v = 10$ mV s^{-1}. (A) CV in scanning from −0.3 V after adsorption of the variant at the open circuit potential. The gray line is the first scan, and the dashed black line is the second scan. (B) CV in scanning from −0.1 V. The other conditions are identical with those of (A). (C) CV after adsorption of the variant at 0.5 V. The other conditions are identical with those of (B). (D) CV after the following treatments: the variant was adsorbed at the open circuit potential, and the potential was scanned 2 cycles from −0.1 V to 0.5 V. Thereafter, the electrode was held at −0.3 V for 5 min, and then transferred to a fresh electrochemical solution (McB, pH 4.5) containing 0.2 M D-fructose.

The positively and negatively charged amino acid residues almost homogeneously distribute on the surface of FDH (Fig. 5). In addition, hydrophobic and hydrophilic residues also distribute homogeneously (Fig. 6). These properties seem to lead to random orientation of recombinant (native) FDH on Au electrodes, although the author has to also consider some other contributions from 2-mercaptoethanol[39] and TritonX-100[43] on the orientation for further discussion.
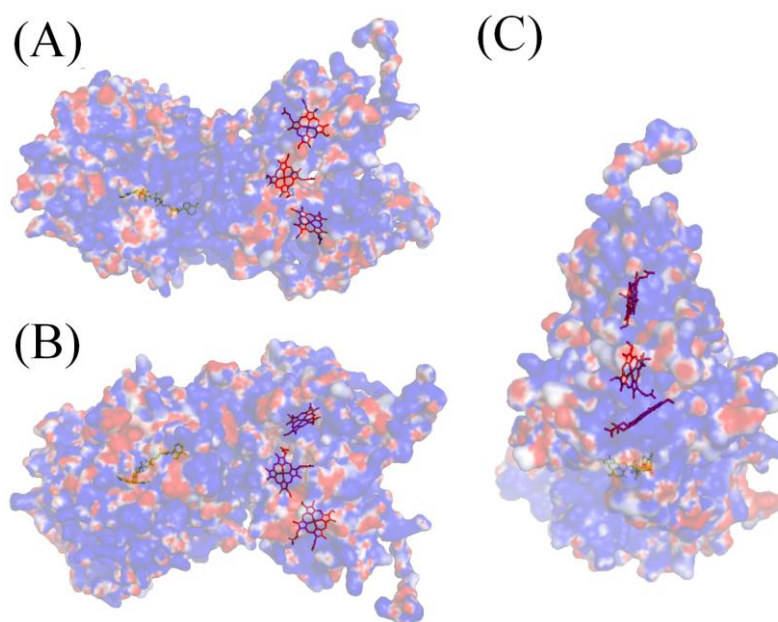
Figure 5. (A): Electrostatic characteristics of the protein surface of FDH. Positive potentials are drawn in blue, negative potentials in red. Heme 1*c*, 3*c*, and 2*c* locate from the top to bottom. (B): After rotation around the horizontal axis by 180° from (A). (C): After rotation around the vertical axis by 90° from (A).
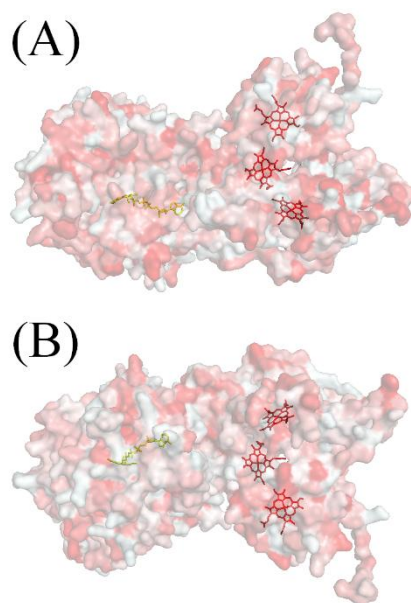
Figure 6. (A): Surface hydrophobicity of FDH. Hydrophobic residues are highlighted in red, hydrophilic in white. Heme $1c$, $3c$, and $2c$ locate from the top to bottom. (B): After rotation around the horizontal axis by 180° from (A). This crystal structure model does not have CHR because the template protein does not have CHR. However, CHR seems not to play significant role in DET-type bioelectrocatalysis, because ΔchrFDH (lacking CHR) show clear DET-type catalytic wave according to previous research.
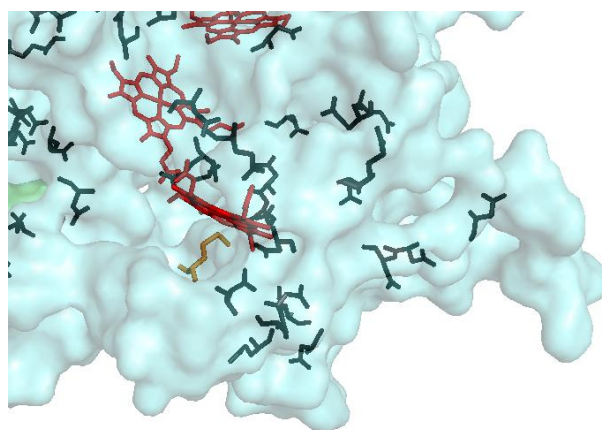

Figure 7. Negatively charged amino acid residues around heme $2c$. Negative charged amino acid residues (Glu and Asp) are drawn in black, Met450 in orange.

On the other hand, the M450Q mutation (for M450QΔ1cFDH and M450Q) was introduced near heme 2c. Several negatively charged amino acid residues such as Glu and Asp exist around heme 2c (Fig. 7). Therefore, it may be considered that the M450Q mutation induces the electrostatic repulsion between Glu at 450 and the other negatively charged amino acid residues around heme 2c, which causes slight change in the conformation to increase the negative potential charge on the surface near heme 2c. Since the heme 2c moiety in M450QΔ1cFDH and M450Q is considered to face to the electrode surface rather homogeneously (Fig. 1(B), some electrostatic repulsion may cause partial desorption from the electrode at negative potentials. However, the adsorbed M450QΔ1cFDH and M450Q are stabilized at positive potentials.

Effects of the protein engineering on the enzyme stability were investigated by recording j_{lim} every one hour at 0.5 V as a measure of the stability. Fig. 8 shows the normalized values of j_{lim} observed at the recombinant (native) FDH- and M450QΔ1cFDH -adsorbed electrode in the presence of D-fructose. The j_{lim} of the recombinant (native) FDH- and M450QΔ1cFDH-adsorbed electrode decreased with time approximately 1% and 8% per hour, respectively. The two mutations resulted in a slight decrease in the stability of the enzyme, although they improved the bioelectrocatalytic property of the enzyme. The M450QΔ1cFDH mutation would disturb the balance between hydrophobic and hydrophilic properties on the enzyme surface, which may causes some structural change in the variant.
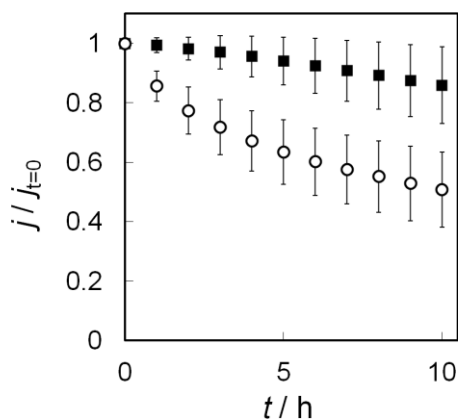

Figure 8. Stability of the recombinant (native) FDH (closed squares) and M450QΔ1cFDH (open circles) adsorbed on bare Au electrodes at 25 °C in McB (pH 4.5) in the presence of 0.2 M D-fructose. The normalized values of j_{lim} obtained from the second cycle CVs taken every

The author performs a kinetic analysis of the catalytic wave on a steady-state catalytic wave considering random orientation of the enzymes. A steady-state model without the concentration polarization of the substrate was used. The following equitation is given to this model [40, 43]:

$$\frac{j}{j_{\text{lim}}} = \frac{1}{\beta\Delta d\left(1 + \exp\left\{\frac{n_{\text{E}}F}{RT}(E - E^{\circ\prime})\right\}\right)}$$

$$\times \ln\left|\frac{\left(1+\exp\left\{\frac{n_{\text{E}}F}{RT}(E-E^{\circ\prime})\right\}\right)+\frac{k_{\text{cat}}}{k^{\circ}_{\text{max}}}\exp\left\{\frac{\alpha n_{\text{E}}F}{RT}(E-E^{\circ\prime})\right\}}{\exp(-\beta\Delta d)\left(1+\exp\left\{\frac{n_{\text{E}}F}{RT}(E-E^{\circ\prime})\right\}\right)+\frac{k_{\text{cat}}}{k^{\circ}_{\text{max}}}\exp\left\{\frac{\alpha n_{\text{E}}F}{RT}(E^{\circ\prime}-E^{\circ\prime})\right\}}\right| \quad (2)$$

where n_{E} is the number of electrons in the rate determining step of the interfacial electron transfer process (=1 in this case since the number of the electron for the heme c); F, Faraday constant; R, the gas constant; T, the absolute temperature; k°_{max}, the standard rate constant at the closest approach in the best orientation of the enzyme; Δd, the distance between the closest and farthest approach of the enzyme; α, the transfer coefficient; β, the coefficient in the long range electron transfer; $E^{\circ\prime}$, the formal potential of the redox center of the enzyme for electrochemical communication with electrode.

The limited current density (j_{lim}) value completely controlled by the enzyme kinetics is expressed by the equation (1). Eqs. (1) and (2) were fitted to the wave of the forward scan at the M450QFDH- and M450QΔ1cFDH-adsorbed electrode using nonlinear regression analysis by a free soft GNUPLOT with $k_{\text{cat}}/k^{\circ}_{\text{max}}$, $\beta\Delta d$, and $E^{\circ\prime}$ as adjustable parameters by setting $j_{\text{lim}}=j_{0.5\text{ V}}$ and α=0.5. The waves of the forward scan at the recombinant (native) FDH- and Δ1cFDH-adsorbed electrodes were also analyzed in the same manner, but $k_{\text{cat}}\Gamma_{\text{eff}}$ was also used as an adjustable parameter, because clear limiting current could not be obtained at 0.5 V. At more positive potentials than 0.5 V the catalytic currents decreased due to the formation of Au oxide layer [42].

Fig. 9 shows the steady-state volammograms at recombinant (native) FDH- and variants-adsorbed electrode in McB (pH4.5) in the presence of 0.2 M D-fructose under anaerobic conditions. The scan rate was 10 mV s^{-1}. The error bars were evaluated by the Student t-distribution at a 90% confidence. Each experimental voltammogram was well reproduced as shown by the dashed lines in Fig. 9. The evaluated values of the fitting parameters of each enzyme-adsorbed electrode were given in Table2.

The $E^{\circ\prime}$ values at M450QFDH- and M450QΔ1cFDH-adsorbed electrode were more negative than those at recombinant (native) FDH- and Δ1cFDH-adsorved electrode respectively, as the author expected. This date support the negative direction shifts of $E_{1/2}$ due to the electron-donating character of methionine ligand.

The $k_{cat}/k°_{max}$ values at M450QFDH- and M450QΔ1cFDH-adsorbed electrode were much smaller than those at recombinant (native) FDH- and Δ1cFDH-adsorved electrode respectively. On the other hand, the $k_{cat}/k°_{max}$ values at Δ1cFDH- and M450QΔ1cFDH-adsorbed electrode were slightly smaller than those at recombinant (native) FDH- and M450QFDH-adsorved electrode respectively. k_{cat} is different from the solution activity that depends on electron acceptors. However, in order to discuss $k°_{max}$ value, the author may assume that k_{cat} is proportional to the solution activity of a given electron acceptor. On the assumption, it is expected that the assumed $k°_{max}$ values at M450QFDH- and M450QΔ1cFDH-adsorbed electrode were 11 times and 27 times larger than those at recombinant (native) FDH- and Δ1cFDH-adsorved electrode respectively. M450QFDH and M450QΔ1cFDH are adsorbed on Au electrode more suitable for DET-type bioelectrocatalysis than recombinant (native) FDH and Δ1cFDH. In contrast, the assumed $k°_{max}$ values at Δ1cFDH- and M450QΔ1cFDH-adsorbed electrode were 1.2 times and 2.9 times larger than those at recombinant (native) FDH- and M450QFDH-adsorved electrode respectively. The effect of Δ1c mutation on the adsorption orientation of variants is very small.

In case of $\beta\Delta d$, the calculated Δd values by using the reported value of β for proteins (approximately 1.4 Å^{-1} [47]) are within a range from 5.1 to 6.0 Å. Considering the diameter of FDH (70 Å) evaluated by atomic force microscopy [48], $\beta\Delta d$ is almost independent of the mutations. The results indicate that the extent of the random orientation seems to be similar each variants.
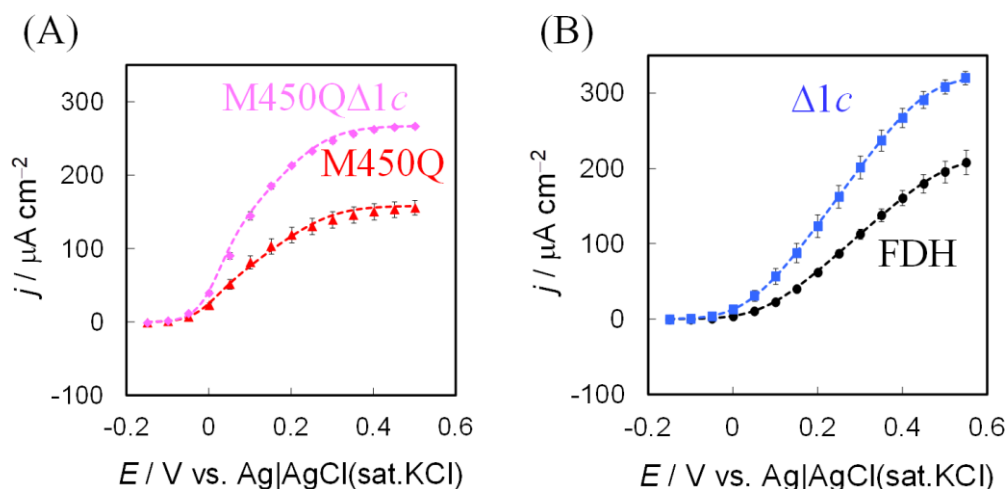
Figure 9. Steady-state voltammograms of D-fructose oxidation at (A) M450QΔ1*c*FDH- (pink diamond) and M450QFDH- (red triangle) adsorbed electrode and (B) Δ1*c*FDH- (blue square) and the recombinant (native) FDH- (black circle) adsorbed electrodes in McB (pH4.5) in the presence of 0.2 M D-fructose under anaerobic conditions. The scan rate was 10 mV s^{-1}. The error bars were evaluated by the Student *t*-distribution at a 90% confidence. Each dashed line indicates the regression result estimated according to Eqs. (1) and (2).

variants	$E^{\circ\prime}$ / mV	k_{cat}/k°_{max}	$\beta\Delta d$	$k_{cat}\Gamma_{eff}$ / nmol cm^{-2} s^{-1}
(native) FDH	30.4 ± 0.6	2.62 ± 0.06	8.22 ± 0.07	1.11 ± 0.01
Δ1*c*FDH	19.3 ± 0.2	1.26 ± 0.02	8.47 ± 0.04	1.68 ± 0.01
M450QFDH	14.3 ± 0.3	0.19 ± 0.01	7.2 ± 0.1	0.818 ± 0.08 (fixed)
M450QΔ1*c*FDH	18.1 ± 0.3	0.049 ± 0.008	8.0 ± 0.2	1.38 ± 0.02 (fixed)

Table 2 Properties of the recombinant (native) FDH and variants.

Conclusions

The author has successfully constructed and purified a variant of M450QΔ1*c*FDH that lacks 143 amino acid residues involving the heme 1*c* moiety and has glutamine in place of methionine as the sixth axial ligand of heme 2*c*. The linear sweep voltammogram of D-fructose oxidation at M450QΔ1*c*FDH-adsorbed electrode exhibited a large limited current density and a negative direction shift of $E_{1/2}$ compared to that at the recombinant (native) FDH-adsorbed electrode. Moreover, it is suggested that the M450QΔ1*c*FDH is rather homogeneously adsorbed in orientations suitable for DET-type bioelectrocatalysis. It is considered that the negative direction shift of $E_{1/2}$ is attributed to a negative direction shift of the redox potential of heme 2*c* as the electron-donating site

in the DET reactions and to the improved interfacial electron transfer kinetics due to homogeneous orientation suitable for DET reactions. The large current is attributed to an increase in the surface concentration of the enzyme on an electrode due to downsizing. This is the first report to support the idea that the effects of the two types of the mutations are rather simply additive even under drastic mutation. Unexpected but effective effect of the mutation is that the variants with M450Q stably and homogeneously adsorb at positively charged electrode surface compared with the recombinant (native) FDH and Δ1*c*FDH. Therefore, the strategy of mixed type mutations is useful for improving the properties of the DET-type bioelectrocatalysis of other redox enzymes, and the variant may be applicable to constructing high power biofuel cells and sensitive biosensors under suitable conditions. Further strategy of the mutation required in future will be to improve the stabilization.

References

[1]   S.V. Hexter, T.F. Esterle, F.A. Armstrong, A unified model for surface electrocatalysis based on observations with enzymes, Phys. Chem. Chem. Phys. 16 (2014) 11822

[2]   C. Léger, P. Bertrand, Direct electrochemistry of redox enzymes as a tool for mechanistic studies, Chem. Rev. 108 (2008) 2379.

[3]   R.D. Milton, S.D. Minteer, Direct enzymatic bioelectrocatalysis: differentiating between myth and reality, J. R. Soc. Interface, 14 (2017) 0253.

[4]   N. Mano, A. de Poulpiqet, O2 reduction in enzymatic biofuel cells, Chem. Rev., 118 (2018) 2392.

[5]   D. Leech, P. Kavanagh, W. Schuhmann, Enzymatic fuel cells: recent progress, Electrochim. Acta. 84 (2012) 223.

[6]   S.C. Barton, J. Gallaway, P. Atanassov, Enzymatic biofuel cells for implantable and microscale devices, Chem. Rev. 104 (2004) 4867.

[7]   S. Shleev, J. Tkac, A. Christenson, T. Ruzgas, A.I. Yaropolov, J.W. Whittaker, L. Gorton, Cellobiose dehydrogenase modified electrodes: advances by materials science and biochemical engineering, Anal. Bioanal. Chem. 405 (2013) 3637.

[8]   N. Mano, L. Edembe, Bilirubin oxidases in bioelectrochemistry: Features and recent findings, Biosens. Bioelectron. 50 (2013) 478

[9]   M. Sensi, M. del Barrio, C. Baffert, V. Fourmond, C. Léger, New perspectives in hydrogenase direct electrochemistry, Curr. Opin. Electrochem. 5 (2017) 135.

[10]   I. Mazurenko, X. Wang, A. de Poulpiquet, E. Lojou, H2/O2 enzymatic fuel cells: from proof-of-concept to powerful devices, Sustainable Energy Fuels, 1 (2017) 1475.

[11]   K. Sakai, H. Xia, Y. Kitazumi, O. Shirai, K. Kano, Assembly of Direct-Electron-Transfer-Type Bioelectrodes with High Performance, Electrochim. Acta. 271 (2018) 271.

[12] W. Zhang, G. Li, Third-generation biosensors based on the direct electron transfer of proteins, Anal. Aci. 20 (2004) 603.

[13] T. Ikeda, Bioelectrochemical studies based on enzyme-electrocatalysis, Electrochim. Acta. 82 (2012) 158.

[14] A.A. Karyakin, Principles of direct (mediator free) bioelectrocatalysis, Bioelectrochemistry 88 (2012) 70.

[15] T. Ikeda, F. Matsushita, M. Senda, Amperometroc fructose sensor based on direct bioelectrocatalysis, Biosens. Bioelectron. 6 (1991) 299.

[16] Y. Kamitaka, S. Tsujimura, N. Setoyama, T. Kajino, K. Kano, Fructose/dioxygen biofuel cell based on direct electron transfer-type bioelectrocatalysis, Phys. Chem. Chem. Phys. 9 (2007) 1793.

[17] Y. Kamitaka, S. Tsujimura, K. Kano, High current density bioelectrolysis of D-fructose at fructose dehydrogenase-adsorbed and ketjen black-modified electrodes without a mediator, Chem. Lett. 36 (2007) 218.

[18] H. Xia, Y. Hibino, Y. kitazumi, O. Shirai, K. Kano, Interaction between D-fructose hydrogenase and mthoxy-substituted-functionalized carbon surface to increase productive orientations, Electrochim. Acta. 218 (2016) 41.

[19] P. Bollella, Y. Hibino, K. Kano, L. Gorton, R. Antiochia, The influence of pH and divalent/monovalent cations on the internal electron transfer (IET), enzymatic activity, and structure of fructose dehydrogenase. Anal. Bioanal. Chem., 410 (2018) 3253.

[20] K. So, S. Kawai, Y. Hamano, Y. Kitazumi, O. Shirai, M. Hibi, J. Ogawa, K. Kano, Improvement of a direct electron transfer-type fructose/dioxygen biofuel cell with a substrate-modified miocathode, Phys. Chem. Chem. Phys., 16 (2014) 4823.

[21] M. Ameyama, E. Shinagawa, K. Matsushita, O. Adachi, D-Fructose dehydrogenase of *gluconobacter industrius*: purification, characterization, and application to enzymatic microdetermination of D-fructose, J. Bacteriol. 145 (1981) 814.

[22] S. Kawai, M. Tsutsumi, T. Yakushi, K. Kano, K. Matsushita, Heterologous overexpression and characterization of a flavoprotein-cytochrome *c* complex fructose dehydrogenase of *gluconobacter iapinicus* NBRC3260, Appl. Environ. Microbiol. 79 (2013) 1654.

[23] S. Kawai, T. Yakushi, K. Matsushita, Y. Kitazumi, O. Shirai, K. Kano, The electron transfer pathway in direct electrochemical communication of fructose dehydrogenase with electrodes, Electrochem. Commun, 38 (2014) 28.

[24] Y. Hibino, S. Kawai, Y. Kitazumi, O. Shirai, K. Kano, Mutation of heme c axial ligand in D-fructose dehydrogenase for investigation of electron transfer pathways and reduction of overpotential in direct electron transfer-type bioelectrocatalysis. Electrochem. Commun., 67 (2016) 43.

[25] Y. Hibino, S. Kawai, Y. Kitazumi, O. Shirai, K. Kano, Construction of a protein-engineering variant of d-fructose dehydrogenase for direct electron transfer-type bioelectrocatalysis. Electrochem. Commun., 77 (2017) 112.

[26] G. Güven, R. Prodanovic, U. Schwaneberg, Electroanalysis, Protein Engineering – An Opinion for Enzymatic Biofuel Cell Design, 22 (2010) 765.

[27] K. Kataoka, H. Komori, Y. Ueki, Y. Konno, Y. Kamitaka, S. Kurose, S. Tsujimura, Y. Higuchi, K. Kano, D. Seo, T. Sakurai, Structure and function of the engineered multicopper oxidase CueO from *Escherichia coli* –Deletion of the methionine-rich helical region covering the substrate-binding site, J. Mol. Biol. 373 (2007) 141.

[28] G. Presnova, V. Grigorenko, A. Egorov, T. Ruzgas, A. Lindgren, L. Gorton, T. Börchers, Direct electron transfer of recombinant horseradish peroxidase on gold, Faraday Discus. 116 (2000) 281

[29] O. Courjean, F. Gao, N. Mano, Deglycosylation of glucose oxidase for direct and efficient glucose electrooxidation on a glassy carbon electrode, Angw. Chem., Int. Ed. 48 (2009) 5897

[30] R. Ortiz, H. Matsumura, F. Tasca, K. Zahma, M. Samejima, K. Igarashi, R. Ludwig, L. Gorton, Effect of deglycosylation of cellobiose dehydrogenase on the enhancement of direct electron transfer with electrodes, Anal. Chem. 84 (2012)10315.

[31] G. Battistuzzi, M. Borsari, J.A. Cowan, A. Ranieri, M. Sola, Control of cytochrome c redox potential: axial ligation and protein environment effects, J. Am. Chem. Soc. 124 (2002) 5315.

[32] Y. Kamitaka, S. Tsujimura, K. Kataoka, T. Sakurai, T. Ikeda, K. Kano, Effects of axial ligand mutation of the type I copper site in bilirubin oxidase on direct electron transfer-type bioelectrocatalytic reduction of dioxigen, J. Electroanal. Chem. 601 (2007) 119.

[33] V. Balland, C. Hureau, A. M. Cusano, Y. Liu, T. Tron, B. Limoges, Oriented Immobilization of a Fully Active Monolayer of Histidine-Tagged Recombinant Laccase on Modified Gold Electrodes, Chem. Eur. J., 14 (2008) 7186.

[34] M.E. Kovach, P.H. Elzer, D.S. Hill, G.T. Robertson, M.A. Farris, R.M. Roop, K.M. Peterson, Four new derivatives of the broad-host-range cloning vector pBBR1MCS, carrying different antibiotic-resistance cassettes, Gene 166 (1995) 175.

[35] D.H. Figurski, D.R. Helinski, Replication of an origin-containing derivative of plasmid RK2 dependent on a plasmid function provided in trans, Proc. Natl. Acad. Sci. U. S. A. 76 (1979) 1648.

[36] S.G. Grant, J. Jessee, F.R. Bloom, D. Hanahan, Differential plasmid rescue from transgenic mouse DNAs into *Escherichia coli* methylationrestriction-mutants, *Proc. Natl. Acad. Sci. U. S. A.,* 87 (1990) 4645

[37] H.W. Boyer, D. Roulland-Dussoix, A complementation analysis of the restriction and modification of DNA in *Escherichia coli,. J. Mol. Biol.,* 41 (1969) 459

[38]   H. Habe, Y. Shimada, T. Yakushi, H. Hattori, Y. Ano, T. Fukuoka, D. Kitamoto, M. Itagaki, K. Watanabe, H. Yanagishita, K. Matsushita, K. Sakaki, Microbial production of glyceric acid, an organic acid that can be mass produced from glycerol, *Appl. Environ. Microbiol.,* 75 (2009) 7760

[39]   J. Marcinkeviciene, G. Johansson, Kinetic studies of the active sites functioning in the quinohemoprotein fructose dehydrogenase, FEBS Lett. 318 (1993) 23-26.

[40]   C. Léger, A.K. Jones, S.P.J. Albracht, F.A. Armstrong, Effect of a dispersion of interfacial electron transfer rates on steady state catalytic electron transport in [NiFe]-hydrogenase and other enzymes, J. Phys. Chem. B 106 (2002) 13058.

[41]   C. Léger, A.K. Jones, W. Roseboom, S.P.J. Albracht, F.A. Armstrong, Enzyme electrokinetics: hydrogen evolution and oxidation by *allochromatium vinosum* [NiFe]-hydrogenase, Biochemistry 41 (2002) 15736.

[42]   Y. Sugimoto, Y. Kitazumi, O. Shirai, K. Kano, Role of 2-mercaptoethanol in direct electron transfer-type bioelectrocatalysis of fructose dehydrogenase at Au electrodes, Electrochim. Acta 170 (2015) 242.

[43]   H. Xia, Y. Kitazumi, O. Shirai, K. Kano, Enhanced direct electron transfer-type bioelectrocatalysis of bilirubin oxidase on negatively charged aromatic compound-modified carbon electrode, J. Electroanal. Chem. 763 (2016) 104.

[44]   K. So, Y. Kitazumi, O. Shirai, K. Kano, Analysis of factors governing direct electron transfer-type bioelectrocatalysis of bilirubin oxidase at midified electrodes, J. Electroanal. Chem. 783 (2016) 316.

[45]   Y. Sugimoto, Y. Kitazumi, O. Shirai, K. Kano, Effects of Mesoporous Structures on Direct Electron Transfer-Type Bioelectrocatalysis: Facts and Simulation on a Three-Dimensional Model of Random Orientation of Enzymes, Electrochemistry, 85(2) (2017) 82.

[46]   S. Kawai, T. Yakushi, K. Matsushita, Y. Kitazumi, O. Shirai, K. Kano, Bioelectrochemical characterization of the reconstruction of heterotrimeric fructose dehydrogenase from its subunits, *Electrochim. Acta*, **152**, 194 (2015).

[47]   C.C. Moser, J.M. Keske, K. Warncke, R.S. Farid, P.L. Dutton, Nature of biological electron transfer, Nature 355 (1992) 796–802.

[48]   M. Tominaga, C. Shirakihara, I. Taniguchi, Direct heterogeneous electron transfer reactions and molecular orientation of fructose dehydrogenase adsorbed onto pyrolytic graphite electrodes, *J. Electroanal. Chem.*, 610 (2007) 1

Chapter 4

Ultimate downsizing of D-fructose dehydrogenase for improving the performance of direct electron transfer-type bioelectrocatalysis

D-Fructose dehydrogenase (FDH), a membrane-bound heterotrimeric enzyme, shows strong activity in direct electron transfer (DET)-type bioelectrocatalysis. An FDH variant ($\Delta 1c2c$FDH) which lacks 199 amino acid residues including two heme c moieties from N-terminus was constructed, and its DET-type bioelectrocatalytic performance was evaluated with cyclic voltammetry at Au planar electrodes. A DET-type catalytic current of D-fructose oxidation was clearly observed on $\Delta 1c2c$FDH-adsorbed Au electrodes. Detailed analysis of the steady-state catalytic current indicated that $\Delta 1c2c$FDH transports the electrons to the electrode via heme $3c$ at a more negative potential and at more improved kinetics than the recombinant (native) FDH.

Introduction

Bioelectrocatalysis, which couples the electrode reaction and the catalytic function of the redox enzyme, attracts attention from the view point of environment, energy, and health [1–10]. Especially, direct electron transfer (DET)-type bioelectrocatalysis that directly couples the two reactions plays an important role in constructing mediator-free biofuel cells and biosensors with simplicity and minimum thermodynamic energy loss.

D-Fructose dehydrogenase (FDH) from *Gluconobacter japonicus* NBRC3260 is a heterotrimeric membrane protein consisting of subunit I (67 kDa), II (50 kDa), and III (20 kDa). Subunit I contains a flavin adenine dinucleotide (FAD) as the catalytic center, while subunit II contains three heme c moieties that we call heme $1c$, $2c$, and $3c$ from N-terminus of subunit II [11,12]. FDH catalyzes the oxidization of D-fructose and shows high DET-type bioelectrocatalytic activity [13]. In previous researches in our group, it was pointed out that the electron was transferred from the substrate-reduced FAD, to heme $3c$, heme $2c$, and an electrode, and that heme $1c$ was not involved in the catalytic electron transfer [14]. In addition, an FDH variant in which the region containing the heme $1c$ binding site was largely deleted ($\Delta 1c$FDH) showed an increase in the catalytic current density [15]. This was presumably due to the downsizing of the enzyme, which resulted in an increase of the surface concentration of $\Delta 1c$FDH.

In this study, we constructed an FDH variant which lacks 199 amino acid residues including heme $1c$ and $2c$ moieties ($\Delta 1c2c$FDH, Fig. 1) with the expectations of (1) an increase in the surface concentrations due to the downsizing and (2) the electron transfer from heme $3c$ directly to electrodes. The two expectations may lead to an increase in the limiting current density and the reduction of the over potential for the catalytic oxidation of D-fructose, respectively.

N-Terminal

MRYFRPLSATAMTTVLLLAGTNVRAQ<u>PTEPTPASAHRPSISRGHYLAIAAD</u><mark>CAACH</mark>

<u>NGRDGQFLAGGYAISSPMGNIYSTNITPSKTHGIGNYTLEQFSKALRHGIRADGAQ</u>

<u>YPAMPYDAYNRLTDEDVKSLYAYIMTEVKPVDAPSPKTQLPFPFSIRASLGIWKIAA</u>

<u>IEGKPYVFDHTHNDDWNRGRYLVDELAH</u><mark>CGECH</mark>TPRNFLLAPNQSAYLAGADIGS

WRAPNITNAPQSGIGSWSDQDLFQYLKTGKTAHARAAGPMAEAIEHSLQYLPDAD

SAIVTYLRSVPAKAESGQTVANFEHAGRPSSYSVANANSRRSNSTLTKTTDGAALYF

AV<mark>CASCH</mark>QSDGKGSKDGYYPSLVGNTTTGQLNPNDLIASILYGVDRTTDNHEILMF

AFGPDSLVQPLTDEQIATIADYVLSHFGNAQATVSADAVKQVRAGGKQVPLAKLAS

GVMLLLGTGGILGAILVVAGLWWLISRRKKRSA   **C-Terminal**

Figure 1. The amino acid sequences of subunit II. The underlined amino acid sequences were deleted in Δ1cFDH. The underlined and double underlined amino acid sequences were deleted in Δ1c2cFDH. Three marked amino acid sequences (CXXCH) are motifs for the heme c covalently bound sites. The N-terminal sequences from RYFRP to NVRAQ are the signal peptide that plays a significant role in expression of FDH.

Experimental

Materials

Herculase II fusion DNA polymerase, restriction endnucleases and DNA ligase were purchased from Agilent Technologies (Santa Clara, CA), Takara Shuzo (Japan) and Toyobo (Japan), respectively. Other chemicals were obtained from Wako Pure Chemical Industries (Japan).

Preparation of the mutants and FDH

In the preparation of the Δ1c2cFDH mutant, in-frame deletion was introduced into plasmid pYUF3 [15]. pYUF3 is a vector pT7Blue (Novagen, Merck, USA) into which a 3.5 kbp DNA fragment corresponding to most of subunit I and all of subunit II and III are inserted. Except for the sequence containing heme 1c and heme 2c, pYUF3 was amplified by inverse polymerase chain reaction using herculase II fusion DNA polymerase. The primers used were fdhC_NSTLTKTTD(+) (5′-AATAGTACTCTGACAAAAACAACCGAT-3′) and fdhC_SignalTerminal(−) (5′-TTGCGCCCGTACGTTCGTCCCTGCGAG-3′), and the PCR product was self-ligated by Ligation-High to form pYKF1. Subsequently, PCR was carried out using pYKF1 as a template and primers UF (5′-cggcctcttcgcctattacg-3′) and UR (5′- aggcaccccaggctttacac-3′), and the amplified fragment obtained was treated with *Hin*dIII and *Bam*HI to get a DNA fragment of 2.7 kbp. This DNA fragment was inserted into plasmid pSHO13 treated with *Hin*dIII and *Bam*HI to obtain pYKF2

[12]. Confirmation of nucleotide sequence of Δ1*c*2*c*FDH was entrusted to Fasmac sequencing service (Japan).

Transformation of YKF2 into *G. oxydans* NBRC12528 Δ*adhA*::Km[r] was carried out by a triparental mating method, in which the HB101 strain carrying pRK2013 was used as a helper strain [16]. According to the literature [12], *Gluconobacter* cells were cultivated, with little modifications. Elution of the Δ1*c*2*c*FDH mutant from DEAE-Sepharose was performed by concentration gradient of McIlvaine buffer (McB) from 20-fold McB to 4-fold diluted McB containing 1 mM 2-mercaptoethanol and 0.1% (w/v) Triton X-100. Recombinant (native) FDH and Δ1*c*FDH were also expressed and purified in the same manner [12,15].

Sodium dodecyl sulfate-polyacrylamide gel electrophoresis (SDS-PAGE) was performed using 12.5% acrylamide gel at 100 V at room temperature, and then proteins and heme *c* were stained by Coomassie Brilliant Blue and 3,3′,5,5′-tetramethylbenzidine, respectively.

Strain	Description	Source or reference
Escherichia coli		
DH5α	F$^-$*endA1hsdR17(r_k^- m_k^+)supE44thi-1λ$^-$recA1gyrA96relA1 deoRΔ(lacZYA-argF)*U169Φ80d*lacZ*ΔM15	[17]
HB101	F$^-$*thi-1 hsdS20*($r_B$$m_B$)*supE44recA13ara14leuB6proA2 lacY1galK2rpsL20*(Str^r*xyl-5 mtl-1λ$^-$)	[18]
Gruconobacter oxydans		
NBRC12528 Δ*adh*A mutant	NBRC12528 Δ*adh*A::Km[r]	[19]

Plasmid	Description	Source or reference
pKR2013	Plasmid mediates plasmid transfer; Km^r	[16]
pT7Blue	General purpose cloning vector	Novagen
pBBR1MCS-4	Broad-host-range plasmid; *mob* Ap^r	[20]
pYUF3	pT7Blue,a 3.5-kb fragment corresponding to most of subunit I and all of subunit II and III of the *fdh$_{ATG}$* genes	[15]
pSHO13	pBBR1MCS-4,a 3.7-kb fragment of the *fdh$_{ATG}$* genes, a 0.7-kb fragment a putative promoter region of the *adhAB* gene of *G.*oxydans621H	[12]
pYKF1	pT7Blue,a 2.7-kb fragment of the *fdh$_{ATG}$* genes lacks 199 amino acids residues including heme 1*c* and 2*c* moieties, a 0.7-kb fragment a putative promoter region of the *adhAB* gene of *G.*oxydans621H	This study

| pYKF2 | pBBR1MCS-4,a 2.9-kb fragment of the *fdh_ATG* genes lacks 199 amino acids residues including heme 1*c* and 2*c* moieties, a 0.7-kb fragment a putative promoter region of the *adhAB* gene of *G.oxydans*621H | This study |

Table 1. Bacterial strains and plasmids used in this study

Electrochemical measurements

Cyclic voltammetry was performed with an ALS1000 electrochemical analyzer at a scan rate (v) of 10 mV s^{-1} (unless otherwise stated) and at 25 °C under anaerobic conditions in McB (pH 4.5). The working electrode was an Au planar disk electrode (3-mm diameter), which was polished to a mirror-like finish with Al$_2$O$_3$ powder (0.05-µm particle size), rinsed with distilled water, and sonicated in distilled water. The reference and counter electrodes were handmade Ag|AgCl|sat.KCl and Pt wire, respectively. A 3 µL aliquot of each enzyme solution was added to the buffer solution for measurements of bioelectrocatalytic currents. In this paper, all the potentials are referred to the reference electrode.

ESR spectroscopy

Electron spin resonance (ESR) spectra were recorded on JES-FA100 (JEOL, Japan), using a glass capillary cell with an inner diameter of 0.5 mm. The microwave power was set to 2 mW. The Δ1*c*2*c*FDH solution was concentrated to 20 µM for the measurements.

Other analytical methods

Enzyme activity was measured spectrophotometrically using potassium ferricyanide (as an electron acceptor) and the ferric dupanol reagent, as described in the literature [11].

Results and discussion

We constructed and purified Δ1*c*2*c*FDH. The SDS-PAGE results showed that Δ1*c*2*c*FDH was satisfactorily purified, and subunit II was reduced in size from 51 kDa to 20 kDa (Fig. 2), which is consistent with that predicted by the protein engineering. The heme-based enzyme concentrations were determined by spectrophotometric measurements using the molar extinction coefficient of the reduced heme *c* at 550 nm ($\varepsilon_{550\,nm} = 23000\,M^{-1}\,cm^{-1}$ [21]), considering that the recombinant (native) FDH, Δ1*c*FDH, and Δ1*c*2*c*FDH have three, two, and one heme *c* moiety (moieties), respectively. The activities of the recombinant (native) FDH, Δ1*c*FDH, and Δ1*c*2*c*FDH were evaluated to be 2.0×10^{10} U mol^{-1}, 1.2×10^{10} U mol^{-1}, and 3.0×10^{9} U mol^{-1}, respectively.
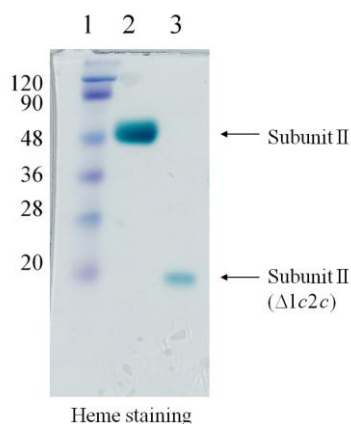
Figure 2. SDS-PAGE photograph of the purified recombinant (native) FDH and a variant. heme *c* moieties in Subunit II are stained by 3,3',5,5'-tetramethylbenzidine. Lane 1, Molecular mass standard (sizes in kDa are shown on the left); Lane 2, recombinant (native) FDH, Lane3, Δ1*c*2*c*FDH

Fig. 3 (A) shows cyclic voltammograms (CVs) measured in the presence of D-fructose with the Au electrodes on which the recombinant (native) FDH, Δ1*c*FDH, and Δ1*c*2*c*FDH were adsorbed. A clear DET-type catalytic wave attributed to the D-fructose oxidation was observed at all of the enzyme-adsorbed electrodes. These waves were independent of the scan rate (from 1 to 50 mV s^{-1}) and the rotating speed (from 0 to 4000 rpm), indicating that the catalytic currents were independent of the mass transfer of the substrate due to a high concentration of the substrate and were controlled by the interfacial electron transfer kinetics and the enzyme kinetics [22-26].

The CVs were normalized against the current density at 0.5 V ($j_{0.5\,V}$), as shown in Fig. 3 (B). The half-wave potential of the steady-state catalytic wave at the Δ1*c*2*c*FDH-adsorbed electrode was approximately 0.19 V and 0.16 V more negative than that of the recombinant (native) FDH-adsorbed electrode and Δ1*c*FDH-adsorbed electrode, respectively. Despite the downsizing of the enzyme, the $j_{0.5\,V}$ value at the Δ1*c*2*c*FDH-adsorbed electrode was slightly smaller than that at the recombinant (native) FDH-adsorbed electrode. This may be ascribed to a decrease in the surface concentration of Δ1*c*2*c*FDH probably due to a decrease in the hydrophobic property by the downsizing of the hydrophobic subunit II. Triton X-100 may in part competitively block the adsorption of Δ1*c*2*c*FDH.

Next, ESR measurements were done for Δ1*c*2*c*FDH that was reduced by D-fructose. The two-electron reduced variant yielded a strong isotropic ESR signal of an organic radical at $g \approx 2$ (Fig. 4). This signal is assigned to the FAD semiquinone radical. The data clearly indicate that one of the two electrons in the fully reduced FAD remains on the FAD to generate the semiquinone radical and that the other electron is transferred to heme 3*c* from the fully reduced FAD.

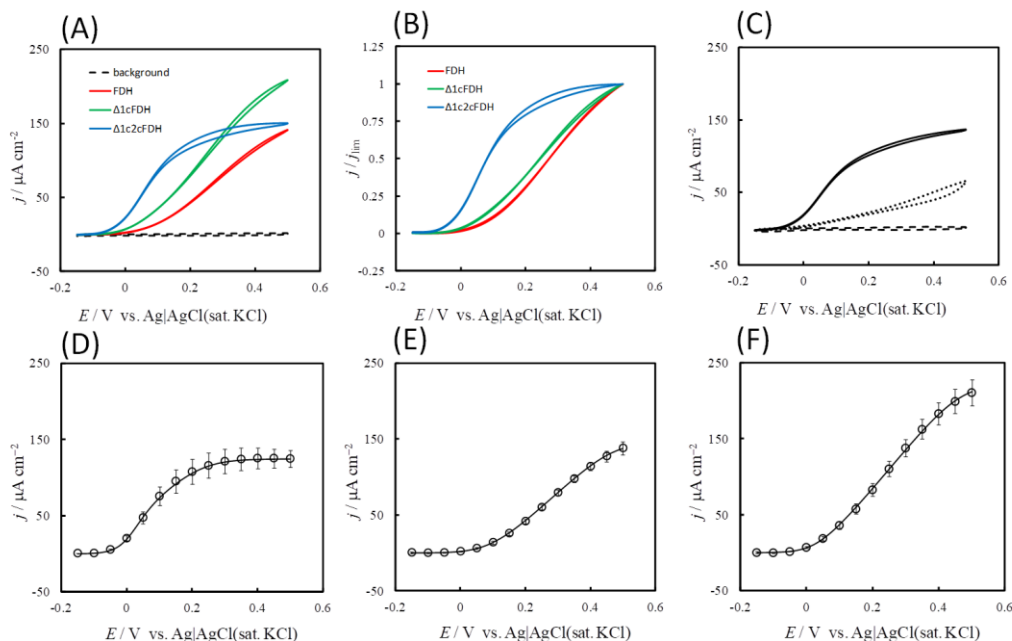Figure 3. (A) Original CVs and (B) normalized CVs of D-fructose oxidation at the recombinant (native) FDH-, $\Delta 1c$FDH-, and $\Delta 1c2c$FDH-adsorbed electrodes in McB (pH 4.5) in the presence of 100 mM D-fructose under anaerobic conditions at $v = 10$ mV s^{-1}. The broken line in panel (A) indicates the background current at the bare Au electrode. In panel (B), the background current was subtracted. In panel (C), the solid line is the CV at the $\Delta 1c2c$FDH-adsorbed electrode in McB (pH 4.5) in the presence of 100 mM D-fructose under anaerobic conditions; the broken line is background, and the dotted line is a CV after the addition of KCN (1 mM in final concentration) at $v = 10$ mV s^{-1}. Panels (D) to (F) show fitted curves obtained by non-linear least square method. The circles are the waves of the forward scan measured with (D) the $\Delta 1c2c$FDH-, (E) recombinant (native) FDH-, and (F) $\Delta 1c$FDH-adsorbed electrodes. The insets indicate the evaluated parameters. The error bars were evaluated by the Student t-distribution at a 90% confidence level.

variants	$E^{\circ\prime}_{\mathrm{enz}}$ / mV	$k_{\mathrm{cat}}/k^{\circ}_{\mathrm{max}}$	Δd	$k_{\mathrm{cat}}\Gamma_{\mathrm{enz,eff}}$ / nmol cm^{-2} s^{-1}
$\Delta 1c2c$FDH	20 ± 1	0.65 ± 0.06	0.454 ± 0.002	0.65 ± 0.06 (fixed)
(native) FDH	54 ± 1	2.44 ± 0.05	0.514 ± 0.002	0.756 ± 0.002
$\Delta 1c$FDH	34 ± 1	1.154 ± 0.007	0.588 ± 0.006	1.154 ± 0.0072 (fixed)

Table 2 Properties of the recombinant (native) FDH and variants. The Δd values were obtained by assuming $\beta = 14$ nm^{-1} [29].

Figure 4. ESR spectrum of D-fructose-reduced state of Δ1c2cFDH at pH 6.0

In addition, in order to clarify the electron transfer pathway in the DET reaction by Δ1c2cFDH, potassium cyanide (KCN) was added to the reaction buffer at a final concentration of 1 mM. The catalytic current density greatly decreased in the presence of KCN, (Fig. 3 (C)). This should be due to the coordination of cyanide ion to the axial ligand of the heme iron, which may cause a redox potential shift of approximately 0.4 V to the negative potential direction [27]. Therefore, the electron transfer from the reduced flavin to the CN$^-$-coordinated heme $3c$ becomes thermodynamically difficult. The very small catalytic wave was observed even in the presence of KCN. The wave showed a residual slope without sigmoidal characteristics, indicating a slow electron transfer kinetics from the CN$^-$-treated Δ1c2cFDH to the electrode [25,26]. The possibility could not be ruled out that the electron might be transferred directly from the reduced FAD to the electrode.

Now, the steady-state catalytic waves were analyzed by considering the random orientation of the enzymes. A steady state model without the concentration polarization of the substrate was used. The following equation is given to this model [23,25]:

$$\frac{j}{j_{\text{lim}}} = \frac{1}{\beta \Delta d \left(1 + \exp\left\{\frac{n_E F}{RT}(E - E^{\circ\prime})\right\}\right)}$$

$$\times \ln \left| \frac{k^{\circ}_{\text{max}}\left(1 + \exp\left\{\frac{n_E F}{RT}(E - E^{\circ\prime})\right\}\right) + k_{\text{cat}} \exp\left\{\frac{\alpha n_E F}{RT}(E - E^{\circ\prime})\right\}}{k^{\circ}_{\text{max}} \exp(-\beta \Delta d)\left(1 + \exp\left\{\frac{n_E F}{RT}(E - E^{\circ\prime})\right\}\right) + k_{\text{cat}} \exp\left\{\frac{\alpha n_E F}{RT}(E - E^{\circ\prime})\right\}} \right| \quad (1)$$

where n_E is the number of electrons in the rate determining step of the interfacial electron transfer process (= 1 in this case since the number of the electron for the heme $3c$ in Δ1c2cFDH); F, Faraday constant; R, the gas constant; T, the absolute temperature; k°_{max}, the standard rate constant at the closest approach in the best orientation of the enzyme; Δd, the distance between the closest and farthest approach of the enzyme; α, the transfer coefficient; β, the coefficient in the long range electron transfer; $E^{\circ\prime}$ the formal potential of the redox center of the enzyme for electrochemical communication with electrode. The limited current density (j_{lim}) value completely controlled by the enzyme kinetics is expressed by the following equation [22–26]:

$$j_{\text{lim}} = n_{\text{S}} F k_{\text{cat}} \Gamma_{\text{eff}} \tag{2}$$

where n_{S} is the number of electrons of the substrate (= 2 in this case); k_{cat}, the catalytic constant; Γ_{eff}, the surface concentration of the effective enzyme immobilized on the electrode.

Equations (1) and (2) were fitted to the wave of the forward scan at the Δ1c2cFDH-adsorbed electrode using nonlinear regression analysis by a free soft GNUPLOT with $k_{\text{cat}} / k^{\circ}_{\text{max}}$, $\beta\Delta d$, and $E^{\circ\prime}$ as adjustable parameters by setting $j_{\text{lim}} = j_{0.5\,\text{V}}$ and α = 0.5 (Fig. 3 (D)). The waves of the forward scan at the recombinant (native) FDH- and Δ1cFDH-adsorbed electrodes were also analyzed in the same manner (Fig. 3 (E, F)), but $k_{\text{cat}}\Gamma_{\text{eff}}$was also used as an adjustable parameter, because clear limiting current could not be obtained at 0.5 V. At more positive potentials than 0.5 V the catalytic currents decreased due to the formation of Au oxide layer [15].

The evaluated values of the fitting parameters of each enzyme-adsorbed electrode were given in Table2). The $k_{\text{cat}} / k^{\circ}_{\text{max}}$ value at the Δ1c2cFDH-adsorbed electrode was much smaller than those at the other electrodes. This is probably because the distance between the active site in the variant and the electrode decreased and k°_{max} increased. The $E^{\circ\prime}$ evaluated for Δ1c2cFDH (20 ± 1 mV) was more negative than those of the recombinant (native) FDH (54 ± 1 mV) and Δ1cFDH (34 ± 1 mV). The data support the electron transfer to the Au electrode from heme 3c for Δ1c2cFDH, while from heme 2c for the recombinant (native) and Δ1cFDH, as illustrated in Fig. 5. The $E^{\circ\prime}$ value for the recombinant (native) FDH was very close to that spectroelectrochemically determined for heme 2c of the enzyme (60 ± 8 mV at pH 5.0) [28], while those of Δ1c2cFDH and Δ1cFDH were slightly more positive than the spectroelectrochemically determined ones of heme 3c (−10 ± 4 mV) and heme 2c for the recombinant (native) FDH. The mutation seems to cause change in the environment around the heme moiety in the variant.

The relative values of $k_{\text{cat}}\Gamma_{\text{eff}}$ were 1 : 1.15 : 1.74 for Δ1c2cFDH-, recombinant (native) FDH, and Δ1cFDH. The value of Γ_{eff} could not be separately evaluated, but was indirectly compared by measuring mediated electron transfer (MET)-type bioelectrocatalytic wave. MET-type-bioelectrocatalytic wave was superimposed on the DET-type wave at potentials more positive than 0.2 V on the addition of $K_4[Fe(CN)_6]$ as a mediator (Fig. 6). The relative heights of the limiting MET-type waves (the remaining limiting currents after subtraction of the DET-type currents) were 1 : 1.1 : 1.8 for Δ1c2cFDH-, recombinant (native) FDH, and Δ1cFDH. The ratio is close to that of $k_{\text{cat}}\Gamma_{\text{eff}}$. Therefore, the ratio of $k_{\text{cat}}\Gamma_{\text{eff}}$ seems to reflect the ratio of Γ_{eff} at almost constant k_{cat}. On the other hand, the mutation did not lead to a big difference in Δd, suggesting that the extent of the random orientation seems to be similar to each other. All these quantitative considerations support the proposed schematic of the productive orientation of the enzymes (Fig. 5).

The increase of $k°_{max}$ in the $\Delta 1c2c$FDH mutant seems to be attributed to a decrease in the distance between the electrochemically communicating heme and the electrode.
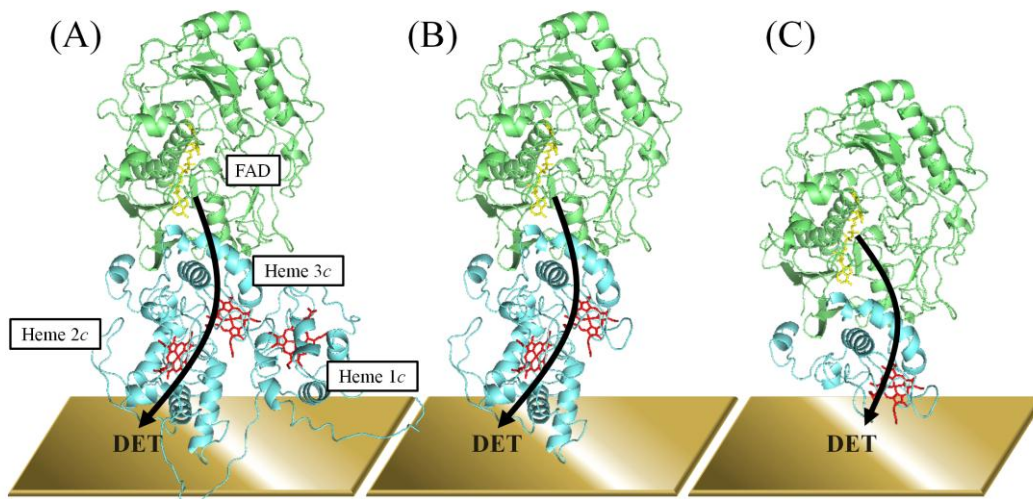

Figure 5. Schematic of orientations suitable for DET-reaction of (A) FDH, (B) $\Delta 1c$FDH, and (C) $\Delta 1c2c$FDH. As templates, FAD-glucose dehydrogenase from *Aspergillus flavus* (PDB 4YNT) and thiosulfate dehydrogenase from *Marichromatium purpuratum* (PDB 5LO9) were used for subunit I (green) and II (cyan), respectively, in the homology modeling [30]. The arrow indicates the presumable pathway of the electron transfer in the DET-type reaction. The subunit III was not shown in the modeling because of lack of the structural information of similar proteins.
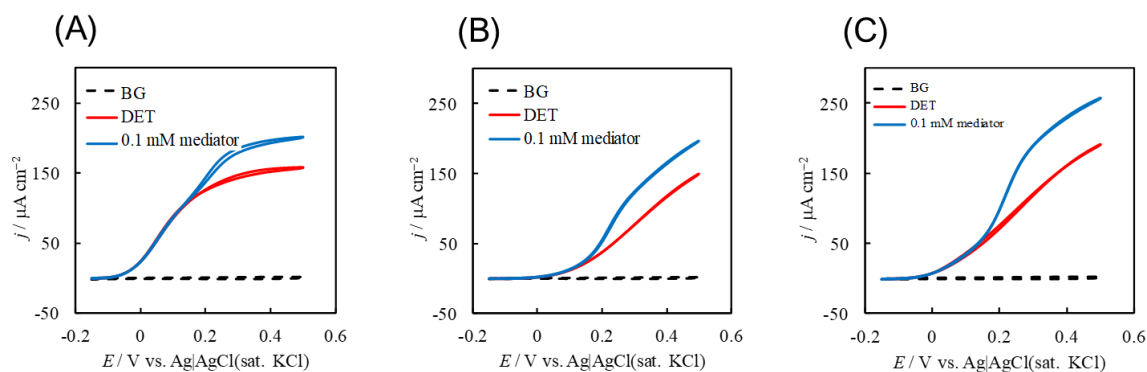
Figure 6. Comparison of MET- and DET-type responses at (A) the $\Delta 1c2c$FDH-, (B) recombinant (native) FDH-, and (C) $\Delta 1c$FDH-adsorbed electrodes. The experimental conditions were identical with those given in Fig. 2 (A), except the presence of 0.1 mM $K_4[Fe(CN)_6]$.

Conclusions

We successfully constructed the $\Delta1c2c$FDH variant that lacks 199 amino acid residues including heme $1c$ and $2c$. The $\Delta1c2c$FDH variant showed bioelectrocatalytic wave for D-fructose oxidation at the planar gold electrode. In the DET reaction of $\Delta1c2c$FDH, the electrons were transferred from D-fructose to the electrode via FAD and heme $3c$ in this order. The $\Delta1c2c$FDH variant transferred the electrons to the electrode at a more negative potential than the recombinant (native) FDH (Fig. 3). Therefore, the energy loss in the DET-type bioelectrocatalysis of FDH successfully decreased. The interfacial electron transfer kinetics were also improved probably by shortening the distance between heme c and the electrode. However, the maximum current density decreased, which is opposite to what we expected from the downsizing mutation. This seems to be due to a decrease in the hydrophobicity of the variant.

References

[1]   N. Mano, A. de Poulpiquet, O$_2$ Reduction in enzymatic biofuel cells, Chem. Rev. 118 (2018) 2392

[2]   I. Mazurenko, A. de Poulpiquet, E. Lojou, Recent developments in high surface area bioelectrodes for enzymatic fuel cells, Curr. Opin. Electrochem. 5 (2017) 74

[3]   K. Kano, T. Ikeda, Fundamentals and practices of mediated bioelectrocatalysis., Anal. Sci. 16 (2000) 1013

[4]   V. Fourmond, C. Léger, Modelling the voltammetry of adsorbed enzymes and molecular catalysts, Curr. Opin. Electrochem. 1 (2017) 110

[5]   J. Wang, Electrochemical glucose biosensors, Chem. Rev. 108 (2007) 814

[6]   C. Léger, P. Bertrand, Direct electrochemistry of redox enzymes as a tool for mechanistic studies, Chem. Rev. 108 (2008) 2379

[7]   D. Leech, P. Kavanagh, W. Schuhmann, Enzymatic fuel cells: Recent progress, Electrochim. Acta. 84 (2012) 223

[8]   F.A. Armstrong, G.S. Wilson, Recent developments in faradaic bioelectrochemistry, Electrochim. Acta. 45 (2000) 2623

[9]   F.A. Armstrong, H.A.O. Hill, N.J. Walton, Direct Electrochemistry of redox proteins, Acc. Chem. Res. 21 (1988) 407

[10]   J.A. Cracknell, K.A. Vincent, F.A. Armstrong, Enzymes as working or inspirational electrocatalysts for fuel cells and electrolysis, Chem. Rev. 108 (2008) 2439

[11]   M. Ameyama, E. Shinagawa, K. Matsushita, O. Adachi, D-fructose dehydrogenase of Gluconobacter industrius: purification, characterization, and application to enzymatic

microdetermination of D-fructose, J. Bacteriol. 145 (1981) 814

[12]   S. Kawai, M. Goda-Tsutsumi, T. Yakushi, K. Kano, K. Matsushita, Heterologous overexpression and characterization of a flavoprotein-cytochrome c complex fructose dehydrogenase of Gluconobacter japonicus NBRC3260, Appl. Environ. Microbiol. 79 (2013) 1654

[13]   T. Ikeda, F. Matsushita, M. Senda, D-fructose dehydrogenase-modified carbon paste electrode containing p-benzoquinone as a mediated amperometric fructose sensor, Agric. Biol. Chem. 54 (1990) 2919

[14]   Y. Hibino, S. Kawai, Y. Kitazumi, O. Shirai, K. Kano, Mutation of heme *c* axial ligands in D-fructose dehydrogenase for investigation of electron transfer pathways and reduction of overpotential in direct electron transfer-type bioelectrocatalysis, Electrochem. Commun. 67 (2016) 43

[15]   Y. Hibino, S. Kawai, Y. Kitazumi, O. Shirai, K. Kano, Construction of a protein-engineered variant of D-fructose dehydrogenase for direct electron transfer-type bioelectrocatalysis, Electrochem. Commun. 77 (2017) 112

[16]   D.H. Figurski, D.R. Helinski, Replication of an origin-containing derivative of plasmid RK2 dependent on a plasmid function provided in trans., Proc. Natl. Acad. Sci. U. S. A. 76 (1979) 1648

[17]   S.G. Grant, J. Jessee, F.R. Bloom, D. Hanahan, Differential plasmid rescue from transgenic mouse DNAs into *Escherichia coli* methylationrestriction-mutants, *Proc. Natl. Acad. Sci. U. S. A.,* 87 (1990) 4645

[18]   H.W. Boyer, D. Roulland-Dussoix, A complementation analysis of the restriction and modification of DNA in *Escherichia coli,. J. Mol. Biol.,* 41 (1969) 459

[19]   H. Habe, Y. Shimada, T. Yakushi, H. Hattori, Y. Ano, T. Fukuoka, D. Kitamoto, M. Itagaki, K. Watanabe, H. Yanagishita, K. Matsushita, K. Sakaki, Microbial production of glyceric acid, an organic acid that can be mass produced from glycerol, *Appl. Environ. Microbiol.,* 75 (2009) 7760

[20]   M.E. Kovach, P.H. Elzer, D.S. Hill, G.T. Robertson, M.A. Farris, R.M. Roop, II, K.M. Petrson, Four new derivatives of the broad-host-range cloning vector pBBR1MCS carrying different antibiotic-resistance cassettes, *Gene*, 166 (1995) 175

[21]   J. Marcinkevicienc, G. Johansson, Kinetic studies of the active sites functioning in the quinohemoprotein fructose dehydrogenase, FEBS Lett. 318 (1993) 23

[22]   K. So, Y. Kitazumi, O. Shirai, K. Kano, Analysis of factors governing direct electron transfer-type bioelectrocatalysis of bilirubin oxidase at modi fi ed electrodes, JEAC. 783 (2016) 316

[23]   H. Xia, Y. Kitazumi, O. Shirai, K. Kano, Enhanced direct electron transfer-type

bioelectrocatalysis of bilirubin oxidase on negatively charged aromatic compound-modified carbon electrode, J. Electroanal. Chem. 763 (2016) 104

[24]   Y. Sugimoto, Y. Kitazumi, O. Shirai, M. Yamamoto, K. Kano, Electrochimica Acta Role of 2-mercaptoethanol in direct electron transfer-type bioelectrocatalysis of fructose dehydrogenase at Au electrodes, Electrochim. Acta. 170 (2015) 242

[25]   C. Léger, A.K. Jones, S.P.J. Albracht, F.A. Armstrong, Effect of a dispersion of interfacial electron transfer rates on steady state catalytic electron transport in [NiFe]-hydrogenase and other enzymes, J. Phys. Chem. B. 106 (2002) 13058

[26]   C. Léger, A.K. Jones, W. Roseboom, S.P.J. Albracht, F.A. Armstrong, Enzyme electrokinetics: Hydrogen evolution and oxidation by Allochromatium vinosum [NiFe]-hydrogenase, Biochemistry. 41 (2002) 15736

[27]   I. Taniguchi, Y. Mie, K. Nishiyama, V. Brabec, O. Novakova, S. Neya, N. Funasaki, Electrochemistry of monoazahemin reconstituted myoglobin at an indium oxide electrode, J. Electroanal. Chem. 420 (1997) 5

[28]   S. Kawai, T. Yakushi, K. Matsushita, Y. Kitazumi, O. Shirai, K. Kano, The electron transfer pathway in direct electrochemical communication of fructose dehydrogenase with Eelectrodes, Electrochem. Commun. 38 (2014) 28–

[29]   C.C. Moser, J.M. Keske, K. Warncke, R.S. Farid, P.L. Dutton, Nature of biological electron transfer, Nature 355 (1992) 796

[30]   P. Bollella, Y. Hibino, K. Kano, L. Gorton, R. Antiochia, The influence of pH and divalent/monovalent cations on the internal electron transfer (IET), enzymatic activity and structure of fructose dehydrogenase, Anal. Bioanal. Chem. 410 (2018) 3253

Conclusion

In this study, the author modified and characterized FDH by the protein engineering techniques, and tried to investigate for the DET-type bioelectrocatalysis reaction of FDH and improve that.

In chapter1, the author constructed the three mutants M301Q, M450Q, and M578Q in which the sixth axial methionine ligand was replaced with glutamine. The cyclic voltammogram (CV) of M301Q (heme 1c modified) was similar to recombinant (native) FDH. Thereby, it is suggested that heme 1c is not involved in the DET-type bioelectrocatalysis. The CV of M450Q (heme 2c modified) was shifted in negative direction and M578Q (heme 3 c modified) drastically decreased DET-type bioelectrocatalytic activity. Therefore, it is suggested that heme 2c is the electron donating site to the electrode, and electrons transfer from FAD to heme 2c via heme 3c. According to these result, electrons transfer as following: FAD $\rightarrow$ heme 3c $\rightarrow$ heme 2c $\rightarrow$ electrode. This conclusion is in agreement with that reported in previous paper. The CV at M450QFDH-adsorved electrode was shifted about 0.2 V in negative direction. This variant is useful for construction of biofuel cell, because it can reduce the overpotential and increase the cell voltage. Additionally, this variant is useful for construction of biosensor, because it is more suitable for operation at 0 V than recombinant (native) FDH and can eliminate noise currents corresponding to directly redox reaction by an electrode such as reduction of oxygen or oxidation of ascorbic acid.

In chapter2, the author constructed a variant of Δ1cFDH that lacks the N-terminus 143 amino acid residues including heme 1c. Δ1cFDH variant retained high DET-type bioelectrocatalytic activity. In addition, the half-wave potential of CV of Δ1cFDH was almost same as that of recombinant (native) FDH. These results supported the electrons transfer pathway concluded in chapter1. On the other hand, Δ1cFDH did not perform *in vivo* catalytic reaction. This result indicates that heme 1c is involved in *in vivo* catalytic reaction, and the electron transfer pathways differ between DET-type bioelectrocatalytic reaction and *in vivo* catalytic reaction. Meanwhile, at Δ1cFDH-adsorved electrode, the limited current density was one and half higher than that of recombinant (native) FDH. This current density increase is corresponding to increase of surface concentration of downsizing engineered enzymes. This variant is remarkably useful for construction of high power density biofuel cell and sensitive biosensor.

In chapter3, the author constructed a variant of M450QΔ1cFDH that lacks 143 amino acid residues involving the heme 1c moiety and has glutamine in place of methionine as the sixth axial ligand of heme 2c. At M450Q- and Δ1cM450Q- adsorbed electrode, the author obtained the limited current independent of electrode voltage in high voltage region. This result indicates that the variants adsorbed on the electrode in the orientation suitable for DET-type bioelectrocatalysis. This result indicate that the negative direction shifts of CV of M450Q and M450QΔ1cFDH are attributed to the

change of formal potential of heme 2*c* and the improved interfacial electron transfer kinetics due to change of adsorption orientation. Additionally, it is suggested that the orientation change was caused by electrostatic interaction between the variants and positive potentials. Meanwhile, At M450QΔ1*c*FDH-adsorved electrode, the linear sweep voltammogram exhibited 1.3 times larger limited current density and 0.2 V lower half wave potential than that at recombinant (native) FDH-adsorved electrode. This is the first report to support the idea that the effects of the two types of the mutations are rather simply additive even under drastic mutation. M450QΔ1*c*FDH is useful variant for construction of large cell voltage, high current density biofuel cell and sensitive, noiseless biosensor. Therefore such conjugation of two type protein engineering strategy is effective of improvement DET-type bioelectrocatalysis.

In chapter4, the author constructed a variant of Δ1*c*2*c*FDH that lacks 199 amino acid residues involving the heme 1*c* and 2*c* moieties. The Δ1*c*2*c*FDH variant showed DET-type bioelectrocatalytic activity in D-fructose oxidation at the planar gold electrode. In the DET-type bioelectrocatalysis of Δ1*c*2*c*FDH, the electrons were transferred from reduced FAD to the electrode via heme 3*c*. Thereby, the Δ1*c*2*c*FDH variant transferred the electrons to the electrode at a more negative potential than the recombinant (native) FDH. Therefore, the overpotential in the DET-type bioelectrocatalysis of FDH successfully decreased. The interfacial electron transfer kinetics was also improved probably by shortening the length between heme *c* and the electrode.

The present works clarified the electron transfer pathway in DET-type bioelectrocatalysis of FDH. Then, this study show the usefulness of protein engineering method considering the electron transfer pathway for improving the properties of the DET-type bioelectrocatalysis of other redox enzymes, and the variant may be applicable to constructing high power biofuel cells and sensitive biosensors under suitable conditions.

Acknowledgement

Acknowledgements

67

The author thanks professors, doctors, and friends, the author have ever met in conferences and events for their kind advices and encouragement.

Finally, the author would like to express his greatest thanks to his family for their continuous encouragement.

<div align="right">

Hibino Yuya

Kyoto

March 2019

</div>

List of Publications

1) <u>Y. Hibino</u>, S. Kawai, Y. Kitazumi, O. Shirai, K. Kano, Mutation of heme c axial ligand in D-fructose dehydrogenase for investigation of electron transfer pathways and reduction of overpotential in direct electron transfer-type bioelectrocatalysis. Electrochem. Commun., 67 (2016) 43-46.
(chapter1)

2) <u>Y. Hibino</u>, S. Kawai, Y. Kitazumi, O. Shirai, K. Kano, Construction of a protein-engineering variant of D-fructose dehydrogenase for direct electron transfer-type bioelectrocatalysis, Electrochem. Commun., 77 (2017) 112-115.
(Chapter2)

3) <u>Y. Hibino</u>, S. Kawai, Y. Kitazumi, O. Shirai, K. Kano, Protein-Engineering Improvement of Direct Electron Transfer-Type Bioelectrocatalytic Properties of D-Fructose Dehydrogenase, Electrochemistry, 87(1) (2019) 47-51
(Chapter3)

4) Y. Kaida, <u>Y. Hibino</u>, Y. Kitazumi, O. Shirai, K. Kano, Ultimate downsizing of D-fructose dehydrogenase for improving the performance of direct electron transfer-type bioelectrocatalysis, Electrochem. Commun., 98 (2019) 101-105
(Chapter4)